Treball de Fi de Master

**Master's degree in Automatic Control and Robotics**

# IDENTIFICATION AND CONTROL OF DC MOTORS

**MEMÒRIA**


**Autor:** Darshan Ramasubramanian
**Director/s:** Dr. Vicenç Puig Cayuela

**Convocatòria:** September 2016


ETSEIB

Escola Tècnica Superior
d'Enginyeria Industrial de Barcelona

UPC

**Abstract**

This work has two main objectives: the first one is identify the model of DC motors - using various techniques from experimental data; Secondly, we want to design appropriate control structures for this system, so as to meet the specifications requested.

The second chapter describes the equipment with which we work throughout the project, consisting of two rotary brushed DC motors provided by the company Ingenia Motion Control. The third chapter describes various techniques of system identification that are used to characterize the motor dynamics, and applied to the motors provided by the company Ingenia Motion Control. And the final chapter covers the design of controllers plants based on the specification in bandwidth, and provides detailed structures of PID control and I-PD control.

This master thesis has been developed in the **Institut de Robòtica i Informàtica Industrial** (IRI) and in the company **Ingenia Motion Control** in the Firmware Division with the supervision of *Vicenç Puig* as director and *Roger Juanpere* and *Rob Verhaart* as advisers from the company.

# Contents

# Chapter 1

# Introduction

A servo drive system is a typical electrodynamic actuator for small high dynamic machine tool axes as well as wire bonding machines and hydraulic/pneumatic valve drives. One of the special servo drive system is the Brushed DC motors. The work is based on the desire to delve into the world of research in the elds of automation and control, applying the knowledge acquired from the Master Course of Automatic Control and Robotics. The main aim of this project is to use the concept of Identification, Simulation and Verification of the model and compare it with the real model environment.

The objective of this project is to analyse the data estimated from the motor, identify the model of the electrical characteristic and mechanical characteristic and verify them in the simulation world with the help of knowledge of control systems. System Identification deals with the problem of building mathematical models of dynamical systems based on observed data from the systems. The subject is part of the basic scientific methodology and since dynamical systems are abundant in our environment, the techniques of system identification have a wide application area.

The methodology is based on results obtained from the simulation of theoretical concepts, which are then validated by repeating experiments on motors. It is very important to do this validation, because sometimes these theoretical concepts are not able to fully capture the nature of the physical elements, and both results may differ. It should be noted that in the course of this project, two rotary Brushed DC motors were the main basis. Proceeding in this way we can guarantee a greater extent that the results are correct.

# Chapter 2

# Background

This chapter discusses the general model and theory behind DC motors, the main importance of the system identification, use of mathematical models and the control laws that are implemented in the motor.

## 2.1 General Description of DC motor

In general, there are two kinds of motors - AC motors and DC motors and in this case, DC motors are the headlines of this project. A DC motors are a part of electrical machines that converts direct current electrical power into mechanical power. These type of motors were the first type widely used, since it could be powered from existing direct-current lighting power distribution systems. A DC motor's speed can be controlled over a wide range, using either a variable supply voltage or by changing the strength of current in its field windings.

There are different kinds of DC motors, such as Stepper motors, Servos, Brushed/Brush-less motors. For a Brushed DC motor, the piece connected to the ground is called the stator and the piece connected to the output shaft is called the rotor. The inputs of the motor are connected to two wires and by applying a voltage across them, the motor turns.

The torque of a motor is generated by a current carrying conductor in a magnetic field. The *Fleming's right-hand rule*, which shows the direction of the induced current when a conductor moves in a magnetic field. It can be used to determine the direction of current in a generator's windings. Using this rule, we can point the right hand fingers in the direction of current, I, and curl them torwards the

direction of magentic flux, B, the direction of force is along the thumb.

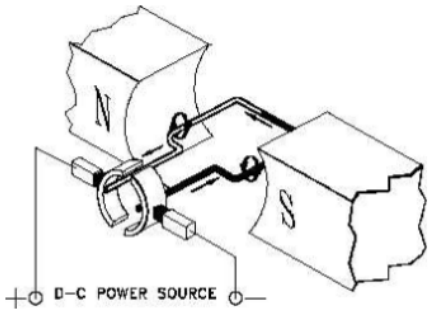


**Figure 2.1:** Construction of Basic DC motor

Now, assume a loop of wire with some resistance is inserted between the two permanent magnets. You might be able to notice that the direction of rotation is changing every half cycle. To keep it rotating in the same direction, it is necessary to switch the current direction. The process of switching the current is called commutation. To switch the direction of current, we have to use the brushes and commutators. Commutation can also be done electronically, in the case of Brushed motors.

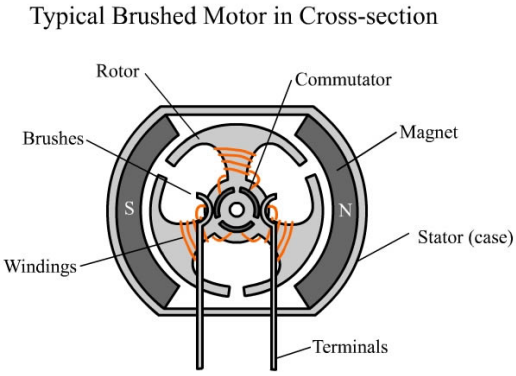


**Figure 2.2:** Working of Brushes and Commutators in DC motors

Based on the description provided above, the mathematical model for the motors will be discussed in the next section, along with the control structure of the model that contains both electrical and mechanical equations of the motor.

## 2.2 Control Structure

The main aim of this section is to define mathematical models, for both current loop and position loop based on the general description from the previous section. The mathematical model was derived from certain equations that are related with working of DC motor.

A mathematical model is a description of a system using mathematical concepts and language. Mathematical models, in general, can take many forms including dynamic systems, differential equations, statistical models, etc. In this case, the goal is to develop the mathematical model for Dynamic system which relates the voltage applied to the armature to the position of the motor.

The set of equations that will be described later in the following subsections, may be represented as nonlinear dynamic system. The main restrictions of this model, with respect to a real motor are

- Assumption that the magnetic circuit is linear
- Assumption that the mechanical friction is only linear in the motor speed.

These restrictions are considered in the identification of the model and based on the restrictions, equations have been derived.

### 2.2.1 Electrical Characteristics

The most important part in this section is the physical reasoning behind the concept of transforming electrical power in mechanical power. As a matter of fact, since the magnetic field $B$ arises from the stator coils, not only the rotor coils may rotate with respect to the stator, but also the stator supply may rotate by increasing the number of coils and by a more sophisticated way. The equivalent electrical circuit is represented below for a DC motor.

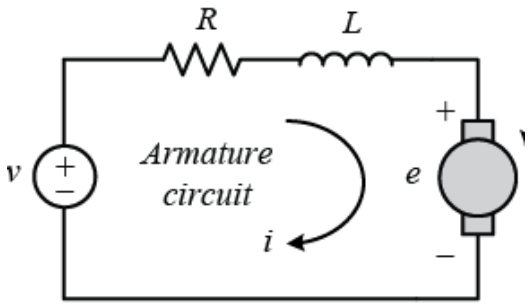


**Figure 2.3:** Electrical Representation of DC motor

Here, the voltage across the coil is represented as $v$ and the armature coil is described by an Inductance ($L$) in series with a Resistance ($R$) which is in series with an induced voltage that opposes the voltage source [9]. The induced voltage is generated by the rotation of the electrical coil through the fixed flux lines of permanent magnets. The equation with such an electric circuit is represented as

$$v(t) = L\frac{di}{dt} + Ri \tag{2.1}$$

Since, the (Eq. 2.1) was assumed to be linear, using the Laplace transform as shown in (Eq. 2.2) we can obtain the transfer function between current and voltage [9].

$$\frac{i(s)}{v(s)} = \frac{K}{\tau s + 1} \tag{2.2}$$

where K = $\frac{1}{R}$ is the stator gain and $\tau$ = $\frac{L}{R}$ is the stator time constant.

Based on the above derivation, we can further deduce the relation between current and torque. For DC motor, Torque is considered as the electromagnetic torque and it varies only with flux $\phi$ and the current I as follows

$$T = k * \phi * I \tag{2.3}$$

### 2.2.2 Mechanical Characterstics

The next important thing is to deal with the mechanical representation of the motor. The below diagram 2.4 shows the model along with the electrical characteristics and it directly provides rotary motion and coupled with wheels or drums, and cables, can provide translational motion.

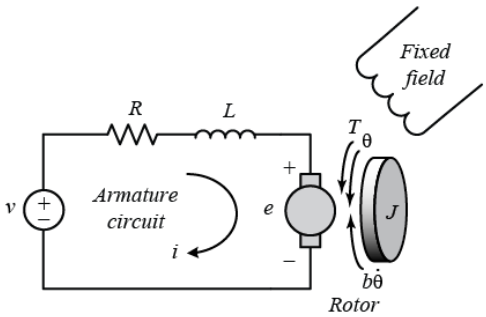


**Figure 2.4:** Mechanical Representation of DC motor

A motor usually exerts a torque, while supplied by voltages on the stator and on the rotor. This torque acts on the mechanical structure, which is characterized by the rotor inertia $J$ and the viscous friction coefficient $B$. The expression that relates the torque and the angular velocity is the following

$$T = K_t * i(t) = J * \frac{dw}{dt} + B * w(t) \tag{2.4}$$

where $K_t$ is the torque constant which relates the current through the torque generated as shown in the article [3]. Since, the velocity of the motor can further deduced into position as follows

$$w(t) = \frac{d\theta(t)}{dt} \tag{2.5}$$

Substituting the (Eq. 2.5) into (Eq. 2.4), it gives

$$K_t * i(t) = J * \frac{d^2\theta(t)}{dt^2} + B * \frac{d\theta(t)}{dt} \tag{2.6}$$

Applying Laplace transformation to the (Eq. 2.6),

$$K_t * i(s) = J * \theta(s) * s^2 + B * \theta(s) * s \tag{2.7}$$

The mechanical model of the motor $G_{motor}$ is defined between the position $\theta(s)$ and the current i(s)

$$G_{motor} = \frac{\theta(s)}{i(s)} = \frac{\frac{K_t}{B}}{s * (\frac{J}{B}s + 1)} \tag{2.8}$$

And this expression can be changed by replacing the terms of $K_t$, $J$ and$B$. Assuming that there is no such values, as manufacturers typically do not provide, must also take into account the own inertia of the load coupled to the motor shaft; its effect can be modeled as a disturbance on the system, which must be corrected by the control loop. Therefore, it ignores these physical parameters and transforms the physical model in a control-oriented model, being

$$G_{motor,pos} = \frac{k}{s(\tau s + 1)} \tag{2.9}$$

The above (Eq. 2.9) represents the model of the position loop and the velocity model can be reduced to by just removing the integrator from the above model being represented as follows

$$G_{motor,vel} = \frac{k}{(\tau s + 1)} \tag{2.10}$$

## 2.3 Control Law

Control theory is an interdisciplinary branch of engineering and mathematics that deals with the behaviour of dynamical systems with inputs, and how their behaviour is modified by feedback. The usual objective of the control theory is to control a plant, which gives an output that follows a control

signal called reference, which maybe a fixed or changing value. For this, it is necessary to design a controller to monitor the output comparing it with the reference. The difference between the actual and desired output, called an error signal, is applied as feedback to the input of the system, to bring the actual output closer to the reference. A block diagram representing the control thoery is represented below in the Figure 2.5.

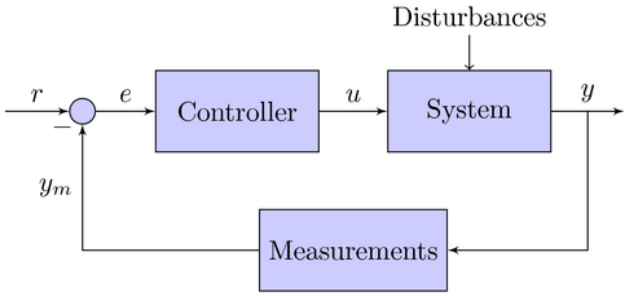


**Figure 2.5:** Block diagram representation of negative feedback control system

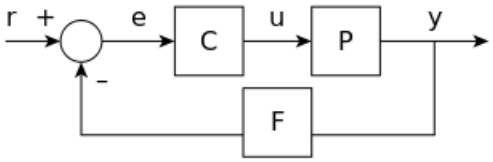


**Figure 2.6:** Block diagram representation of single-input single-output (SISO) system

In general, the Figure 2.6 represents linear and time-invariant system where $C$ is the controller, $P$ is the plant and $F$ is the feedback of the system. The system can be analysed using the Laplace transform on the variables and thus, give the following relations:

$$Y(s) = P(s)U(s) \tag{2.11a}$$

$$U(s) = C(s)E(s) \tag{2.11b}$$

$$E(s) = R(s) - F(s)Y(s) \tag{2.11c}$$

And now solving for Y(s) in terms of R(s), we get

$$Y(s) = \frac{P(s)C(s)}{1 + F(s)P(s)C(s)}R(s) = H(s)R(s) \tag{2.12}$$

This is called the Closed-loop transfer function and in most of the case, $F(s) = 1$. Using the above transfer function method in motor control, it will be a way of designing the controller to achieve and

maintain a goal state by constantly comparing current state with goal state. And the feedback in this case, is given from a sensor feedback. And, the PID controller with or without view modifications is the most common controller used in the servo drives of the motor. For electrical characteristics of the motor, the PI controller was used to make the model stabilize and for the position or velocity loop, PID controller is used as explained in the following sections.

### 2.3.1 PI controller

The Proportional-Integral (PI) algorithm computes and transmits a controller output signal every sample time, $T_s$. PI controller has two tuning parameters to adjust. Integral action enables PI controller to eliminate offset, in case the open loop plant does not contain any integrator, which is a major weakness of P-only controller. Thus, PI controllers provide complexity and capability that makes them by far the most widely used algorithm in process control algorithms.

The controller output is given by

$$K_p e(t) + K_i \int e(t)dt \tag{2.13}$$

where e(t) is the error of deviation of actual measured value from the setpoint.

The lack of derivative action may make the system more steady in the steady state in the case of noisy data. And this type of controller is used to control the current flow in the motors.

### 2.3.2 PID controller

The PID (Proportional-Integral-Derivative) controller is a control loop feedback mechanism which is commonly used in the industrial systems. It continuously calculates an error value as the difference between a desired setpoint and a measured process variable. The controller attempts to minimize the error over time by adjustment of a control variable to a new value determined by a weighted sum:

$$u(t) = K_p e(t) + K_i \int_0^t e(\tau)d\tau + K_d \frac{de(t)}{dt} \tag{2.14}$$

where $K_p$, $K_i$ and $K_d$ denote non-negative coefficients for the proportional, integral and derivative terms respectively.

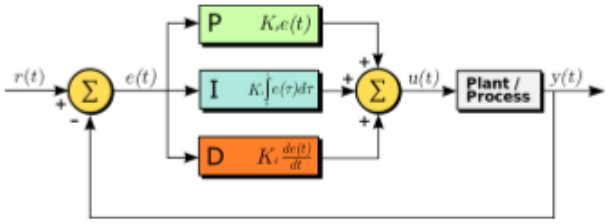


**Figure 2.7:** Block diagram of a PID controller in a feedback loop

### Designing PID controller

In the control of DC motors, a standard specification is based on specifying the bandwidth. This can be by specifying the closed loops through the following procedure:

- Find the transfer function of the system, and express it in terms of the variable s from the Laplace transform, if applicable
- Convert s $\rightarrow$ j$\omega$
- Find the magnitude of the expression obtained in the previous point
- Equal expression of the first magnitude $\frac{1}{\sqrt{2}}$, obtained for the case $\omega = \omega_{BW}$ and solve the resulting equation to find $\omega_{BW}$

As mentioned above, chosen the system presents a unique closed loop pole with multiplicity three. The most general is

$$G_{desired} = \frac{1}{(\tau s + 1)^3} \tag{2.15}$$

Substituting the conversion of s $\rightarrow$ J$\omega$, we get

$$G_{desired} = \frac{1}{(\tau j\omega + 1)^3} \tag{2.16}$$

Now, the magnitude of the $G_{desired}$ is,

$$G_{desired} = \frac{1}{[\sqrt{\tau^2\omega^2 + 1}]^3} \tag{2.17}$$

Equating (Eq. 2.17) to $\frac{1}{\sqrt{2}}$ for $\omega = \omega_{BW}$,

$$\frac{1}{[\sqrt{\tau^2\omega^2 + 1}]^3} = \frac{1}{\sqrt{2}} \tag{2.18}$$

For a simple transfer function of first order model, the poles are:

$$pol = -\frac{1}{\tau} \tag{2.19}$$

Substituting the (Eq. 2.19) in (Eq. 2.18), we get

$$\frac{1}{[\sqrt{\frac{\omega^2}{pol^2} + 1}]^3} = \frac{1}{\sqrt{2}} \tag{2.20}$$

From the equation (Eq. 2.20), we can determine the pol as

$$pol = \pm\frac{\omega_{BW}}{\sqrt{\sqrt[3]{2} - 1}} \tag{2.21}$$

To make the system stable, the poles are placed on the left half plane and thus,

$$pol = -\frac{\omega_{BW}}{\sqrt{\sqrt[3]{2} - 1}} \tag{2.22}$$

Using this above definition of the poles, we can determine the controller gains as discussed in the following chapters.

# Chapter 3

# Real Setup

In this chapter, we will be concentrating on the description of the softwares and the equipments used throughout the project. It shows the systems used in this project, the servo drives, the feedback and the software used to make the system activate. We will also be discussing about the company requirements that they can depend on the project to improve their software.

The main important requirements from the company is to design and identify the model of the motor, collecting data from the software MOTIONLAB and applying it in MATLAB software, where we experiment on the system that will be discussed in the next chapter. MOTIONLAB software is the platform in which all the company's products help improve the system based on the customer requirements. It has various applications that let us configure, program, test and run the drive in a way that are intuitive and simple. And using the features in the software, a tool was designed to determine the data of the motor for the identification of the system. Below Figure 3.1 shows the MOTIONLAB configuration window where the firmware of the identification is uploaded and the identification tool is activated, as seen in the Figure 3.2.

Motors have various applications in the real world, like it can be used in vehicles, cranes, air compressors, conveyors and machines like Weaving machine, Lathe machines, etc. And one of the main applications, that is currently the present and future of science and technology, are the study of Robotics. Motors are generally the motion part of the robots as it is defined in the Section 2.1. In this case, the brushed DC motors are used provided by the company Ingenia Motion Control, namely, **Mot 37** and **Mot 53** as shown in the Figures 3.3 and 3.4 respectively.

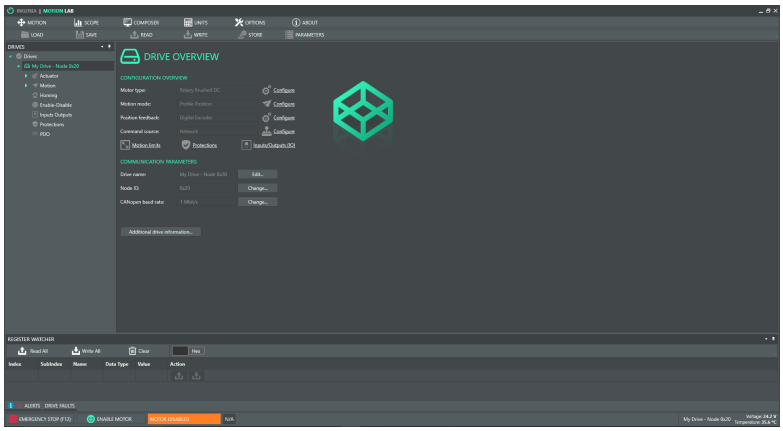


**Figure 3.1:** MotionLab Configuration Window

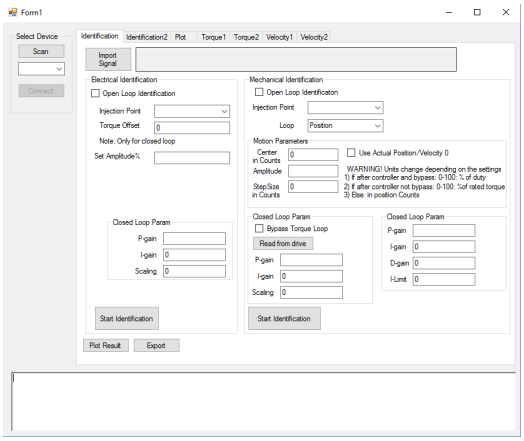


**Figure 3.2:** Identification Tool to collect the datas from the motor

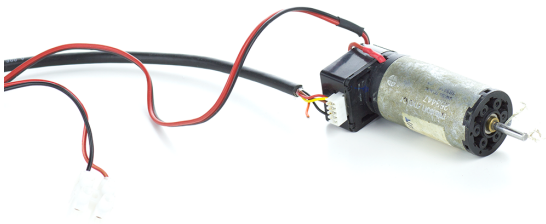

**Figure 3.3:** Motor Mot 37

**Figure 3.4:** Motor Mot 53

The next important part required for this project is the servo drive which acts the communication channel between the motor and the computer. The company provided one of their main servo drive called Pluto Digital Servo Drive, which is shown in the below Figure 3.6. This servo drive is the modular solution for control of rotary or linear brushed DC motors, that works up to 800 W peak, with 8 A continuous output current and no heat sink needed. The controller in the Pluto includes two control loops: one of them made from an electrical point of view - Current; and the other, from a mechanical point of view - Position. Although only mentioned that the work focuses on the bond position, it is considered interesting to show how the two are related ties. Figure 3.5 below shows the connection between these two loops and other elements that make up the system study:

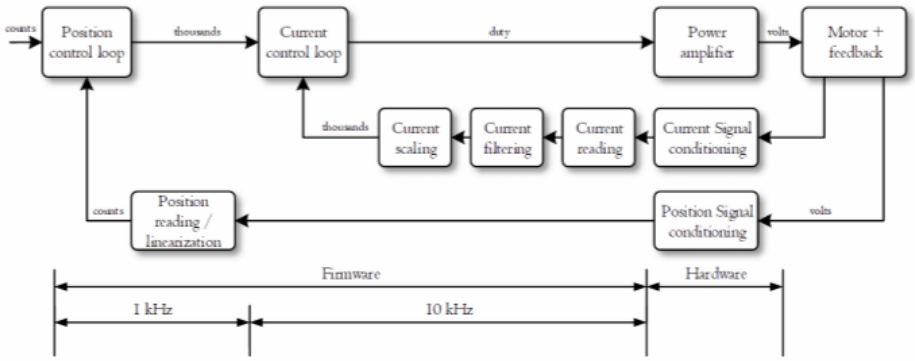


**Figure 3.5:** Block Diagram of the Control Structure of the Pluto

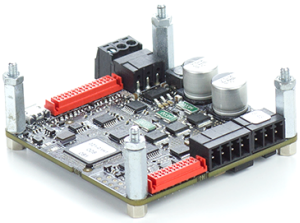

**Figure 3.6:** Pluto Digital Servo drive

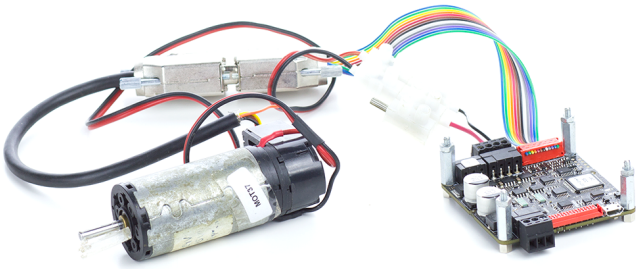

**Figure 3.7:** Setup of the Motor 37

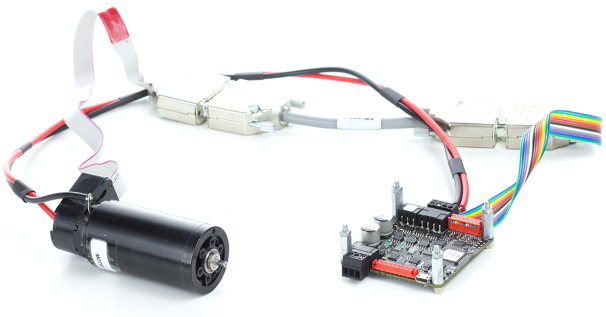

**Figure 3.8:** Setup of the Motor 53

Finally, the last thing needed for the setup of the project is a feedback and a battery supply. Each motor has their own specifications with their own values provided by the manufacturer. The motors that are in use in this project needs a 24 Volts power supply to make the servo drive active, where the data sheet is presented in the Appendix A. And the feedback used here, is a Digital Encoder, for velocity control and/or position control as well as commutation sensor. The encoder provides incremental position feedback that can be extrapolated into precise velocity or position information.

# Chapter 4

# System Identification

This chapter is structured as follows: firstly, the design of input disturbances for the identification, secondly, the analysis of model structures and finally, the electrical identification and the mechanical identification of the motors.

## 4.1 Design of Inputs

This section deals with the input disturbance signal which is the basis for the system identification of both electrical and mechanical part of the motor.

In general, the output can be exactly calculated once the input is known and in most of the cases, this looks unrealistic. Thus, we need some form of disturbances that can be considered as input for a system. Based on these inputs, we calculate the output and use this for identification. And the most important thing here, is to design the input signals. These signals can be either a Sine Sweep, a Psuedo-Random binary noise or a Multisine. And in this case, Multisinus is considered as the natural choice of input, that can be seen in [8], which can be formed as sum of sinusoids

$$u(t) = \sum_{k=1}^{d} a_k cos(w_k t + \varphi_k) \tag{4.1}$$

$$\varphi_k \triangleq \frac{-k.(k-1).\pi}{N} \tag{4.2}$$

$$w_k \triangleq w_{min} + \frac{(k-1).(w_{max} - w_{min})}{N} \tag{4.3}$$

where $a_k$ is the amplitude, $w_k$ is the frequency in rad/s and $\varphi$ is the phase angle.

$$w_{max} = 2\pi f_{max}; w_{min} = 2\pi f_{min}$$

With the above parameters $a_k$ and $w_k$, we can place the signal power very precisely to desired frequencies.

The signal chosen obtains a combination of sinusoidal signals - called Multisinus from now - which covers the frequency spectrum needed for the study.

A specific frequency range has to be mentioned that is required for the operation MATLAB function *msinclip2* used for generating the multisinus. In essence, the operation iterates towards a set of phases to solve the problem of the crest factor, where the algorithm was presented to minimize the peaks of the band limited Fourier signals. This method has the ability to compress the signals effectively without disturbing the spectral magnitudes. The result of this operation is a vector of complex amplitudes of multisinus, which are calculated on a series of operations that lead to the final vector of input values. This entry is to be used to calculate the output.

One of the most important property of this signal is that there is no leakage and thus the periodic signal has a period of $T_0 = 1/f_0$. And the crest factor typically used is 1.7 and we use smaller crest factors to optimize the phases using a numerical optimization routine. These signals can be calculated using Fourier Transformation as mentioned above.

The following sections talks about the frequency resolution and the properties of the signal for Current loop and Position loop respectively.

### 4.1.1 Current Loop

The current loop works with a sampling frequency 10kHz So, the input signal should have a frequency limit of 5kHz and if it goes past this limit, the model unstable and thus we can use the maximum frequency for the identification as 4kHz.

In this case, we can use a lower frequency for the identification but for the current loop, the motor should not move. It is because higher frequency has a lower time constant as it frequency is indirectly proportional to time constant. So, identification is done for the maximum frequency f=4000 Hz and the plot of amplitude vs time is shown in Figure 4.1. Whereas, for the low frequency, the electrical time constant is high enough for the motor to move back and forth as shown in Figure 4.2.

The identification of electrical model is done in both open loop and closed loop to see which provides a better solution, which will be discussed further in the identification of the current loop.

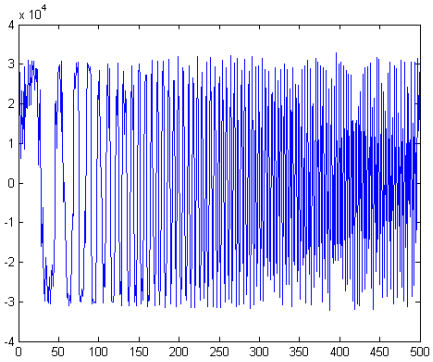


**Figure 4.1:** Multisinus input with frequency f = 4kHz

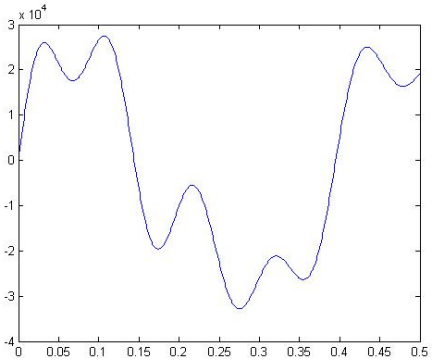


**Figure 4.2:** Multisinus input with frequency f = 100 Hz

For open loop identification, the percentage of amplitude is given as 50% which is common for all the motors because the input is the signal injected and for certain motors, the current flow throughout the model may affect the system and it will be a little difficult to identify the electrical model. The disturbance is measured as percentage of duty cycle and each duty has a maximum limit as follows

$$MaxDuty = 100.\frac{MotorRatedcurrent.MotorResistance}{Voltage} \tag{4.4}$$

For closed loop identification, the percentage of amplitude is given as 10% as the closed loop identification has an offset as the input. This type of identification also involves a controller and the disturbance is added after the controller as described in the later part of this chapter. Here, the disturbance is measured in terms of % of rated torque which can be converted into milli-Newton using the (Eq. 4.5).

$$Torque(mN) = \frac{Torque(\%).RatedTorque(mN)}{1000} \tag{4.5}$$

### 4.1.2 Position Loop

In this section, the main aim is to determine the disturbance signal for the mechanical characteristics of the motor. The position loop works with a sampling frequency of 1 kHz. In this case, the maximum frequency input is 400Hz which is the maximum input for the system identification.

Here, the frequency injected can be of any range that corresponds to the motor requirements and the frequency resolution. Since the maximum frequency that can be injected is 400 Hz, the experiment begins with f = 400 Hz as shown in Figure 4.3.

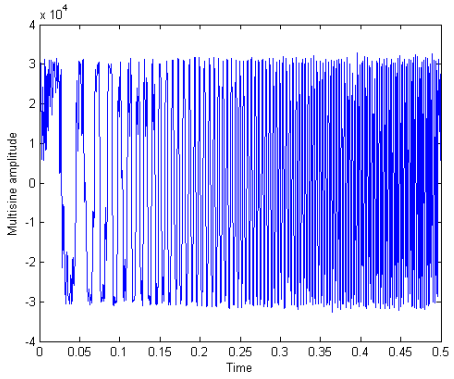


**Figure 4.3:** Multisinus input with frequency f = 400 Hz

For the identification of the position loop, the motor needs to move a step for the identification to be possible, which will be discussed later in this chapter. And thus, the mechanical time constant does not directly depend on the disturbance injected and thus, the frequency can be varied for identifying the model. In this case, the frequencies used are f = 100 Hz and f = 200 Hz apart from the maximum frequency input as shown in Figures 4.4 and 4.5.

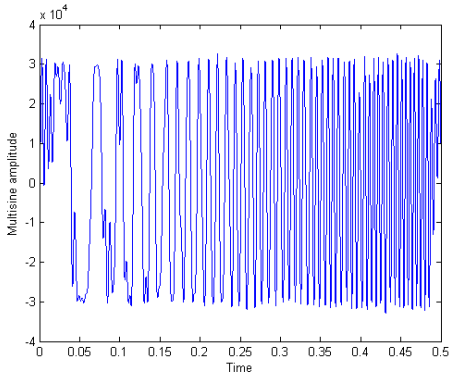


**Figure 4.4:** Multisinus input with frequency f = 200 Hz

Since, the identification can only be done in closed loop for position loop, we set an amplitude for

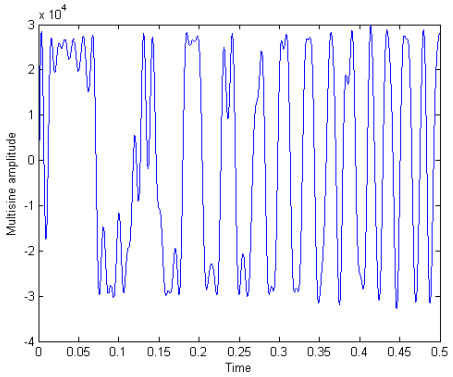


**Figure 4.5:** Multisinus input with frequency f = 100 Hz

the disturbance injected and these amplitudes vary according to the frequency range. For a frequency of f = 400 Hz, the amplitude was given as 20% as the noise occurs in such small time and the higher the amplitude of the disturbance injected for a small time, the easier it will be identify the model of the motor. And similarly, if the frequency range is reduced to f = 100 Hz or 200 Hz, the noise occurs for a long time compared to the high frequency and thus it is advisable to reduce the amplitude but also it is necessary to be high enough to identify the model. Here, the disturbance is measured in % of rated torque as given in (Eq. 4.5), because the output of the controller is the input to the model which contains the electrical model plus the mechanical model as discussed in this chapter.

## 4.2 Analysis of Model Structure

This section contains the information of the model structures that was considered in the PhD thesis [7].

### 4.2.1 Process Models

The Process model, as described in [1], is a simple continuous-time transfer function that describes linear system dynamics which contains the following elements:

- Static Gain $K_p$
- One or more time constants $T_{pk}$
- Process zero $T_z$

The above elements describe specifically the system dynamics that can be used for the identification. The advantages of the model are that they are simple and the model coefficients have an easy interpretation as poles and zeros. There is a possibility to create different model structures by varying the poles, adding an integrator, add a time delay or add a zero. But in this case, the model we describe is either a first order model or first order plus integrator model refer to the motor models presented in the previous chapter.

$$G(s) = \frac{K_p}{\tau_{p1}s + 1} \tag{4.6}$$

$$G(s) = \frac{K_p}{s(\tau_{p1}s + 1)} \tag{4.7}$$

where $K_p$ is the static gain and $\tau_{p1}$ is the time constant.

### 4.2.2 Polynomial model

A polynomial model uses a generalized notion of transfer functions to express the relationship between the input *u(t)*, the output *y(t)* and the noise *e(t)* using the equation:

$$A(q)y(t) = \sum_{i=1}^{nu} \frac{B_i(q)}{F_i(q)} u_i(t - nk_i) + \frac{C(q)}{D(q)} e(t) \tag{4.8}$$

The variables *A*,*B*,*C*,*D*,*F* are the polynomials expressed in the time shift operator $q^{-1}$, $u_i$ is the input at *i*, *nu* is the total number of inputs, and $nk_i$ is the input delay. There are different configurations of polynomial models and those are represented in the following subsections [2].

#### ARX Model

The ARX model (Auto regressive with exogenous terms) is the simplest model that incorporates the stimulus signal. However, this model captures some of the stochastic dynamics as part of the system dynamics. This model is the easiest to estimate since the corresponding estimation problem is of a linear regression type.

$$A(z)y(k) = B(z)u(k - n) + e(k) \tag{4.9}$$

where the *u(k)* is system inputs, *y(k)* is system outputs, *n* is system delay and *e(k)* is system disturbance.

*A(z)* and *B(z)* are polynomial with respect to backward shift operator $z^{-}1$ and defined by the following

$$A(z) = 1 + a_1 z^{-1} + a_2 z^{-2} + ... + a_{k_a} z^{-k_a} \tag{4.10}$$

$$B(z) = b_0 + b_1 z^{-1} + ... + a_{k_b - 1} z^{-(k_b - 1)} \tag{4.11}$$

The identification method of the ARX model is the least squares method, which is special case of the prediction error method.The least squares method is the most efficient polynomial estimation method because this method solves linear regression equations in analytic form and the solution is unique. The foremost disadvantage is that the disturbance model comes along with the system poles and this makes it easier to get an incorrect estimate of the system dynamics because the polynomial A can also include the disturbance properties.

**OE model**

The general linear polynomial model reduces to the output-error model. This model describes the system dynamics separately from the system dynamics. The output-error model does not use any parameters for simulating the disturbance characteristics. The following equation shows the form of the output error model:

$$y(k) = \frac{B(z)}{F(z)} u(k - n) + e(k) \tag{4.12}$$

where the *u(k)* is system inputs, *y(k)* is system outputs, *n* is system delay and *e(k)* is system disturbance.

*B(z)* and *F(z)* are polynomial with respect to backward shift operator $z^{-}1$ and defined by the following equations.

$$B(z) = b_0 + b_1 z^{-1} + ... + a_{k_b - 1} z^{-(k_b - 1)} \tag{4.13}$$

$$F(z) = 1 + f_1 z^{-1} + f_2 z^{-2} + ... + a_{k_f} z^{-k_f} \tag{4.14}$$

The identification method of the output error model is the prediction error method, which is quite similar to ARMAX model structure. If the disturbance *e(k)* is white noise, all minima are global. However, a local minimum can exist if the disturbance is not white noise.

**Conclusion on the Model Structure**

From this section, the process model structure was used for the identification of both current loop and position loop as the order of the model was easy to predict and the identification of the system works better with continuous time than discrete system which will be discussed in the results later in the chapter. The reason to neglect ARX model is because the identified model is actually a predicted model that does not depend directly on the input and output, which might cause some trouble in designing the controller.

## 4.3 Identification methods

This section deals with the concept of System identification for electrical and mechanical loops of the motor. It involves the technique used for injecting the disturbance, analysis of model structures in continuous time and in discrete time, and the representation of mathematical models along with the results.

In general, each object begins and ends with a real data and analysing the data will provide with no desire to move forward in the field of Control systems. And thus, the concept of System Identification can be presented as discussed in the book [4]. System Identification uses statistical methods to build mathematical models from the measured data. The process of converting the data into mathematical models are fundamental in the field of science and engineering and is one of the crucial topics in the Control systems area.

System identification has been an active research area for the past two decades and it has now matured and many techniques have been standardized in the control and signal processing engineering. It also includes the optimal design of experiments to efficiently generate informative data for fitting models as well as model reduction. It is characterized into three categories:

- White-box: It estimates the parameters of the physical model from data
- Grey-box: Using a generic model structure, estimate the parameters from data
- Black-box: Determine model structure and estimate the parameters from data

In general, most of the systems are considered as Black-box models as the only known factors are the real data obtained. It is necessary to analyse various model structures to get a better fit from the

measured data and there are many types of model structures that have been become standard tools in the MATLAB. Using the analysis of model structures from the previous section, the model can be in continuous time and the model structure we can chose is process model as it gives a better fit which will be discussed in the following sections.

### 4.3.1 Electrical Identification

The electrical characteristics of the model was discussed in the previous Chapter 2 and the model is described in the Section 2.2.1 in the (Eq. 2.2) which describes the first order model for the current loop, that contains the variables Inductance ($L$) and Resistance ($R$).

But, there are two methods for identifying the electrical model of the motor and those are:

- Open Loop Identification
- Closed Loop Identification

Both the methods will be discussed in the coming sections along with the results in both time domain and frequency domain.

#### Open loop method

The Open Loop identification method is the simplest and easiest method for the identification of any model. Theoretically, the identification of the model is done between the reference and the Actual output of the real system and a disturbance is applied after the controller to make the system react and then identify the model. This representation is shown in Figure 4.6. In most of the cases, the input is not known and thus it will be difficult to calculate the output of the system. Thus, we use signals that are under our control and determine the output of the system. There are signals that are beyond our control that also affect the system but within our linear framework, we assume to be negligible. Here, the reference is not known and thus the disturbance is designed as mentioned in the previous section and the model was further reduced as shown in Figure 4.7.

The above method was introduced in the MOTIONLAB Identification tool software and the multisinus was introduced with a certain amount of amplitude and applied in the motors which were discussed in the previous Chapter 3.

The amplitude of the signal injected is important for the systems to identify the model. Some systems might not be able to take 100% amplitude and also for safety reasons, we apply 50% signal

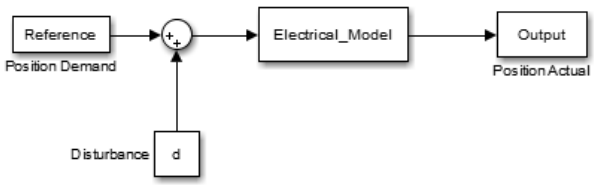


**Figure 4.6:** Open loop System from Reference (Demand) to Output (Actual)

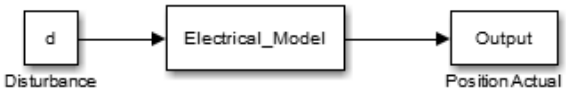


**Figure 4.7:** Open loop System from Disturbance to Output (Actual) reduced from Figure 4.6

amplitude of the Multisinus. As the input signal is injected, the motor gives a small reaction which shows that the motor responds to the input signal. Then the output of the model is taken from software and exported to the MATLAB.

Using the input and output of the system, the model can be identified using the System Identification Application from the MATLAB software. Here, the sampling time given to be $T_s = 0.0001$ seconds.

The next step is to choose the model structure of the system. The easiest way to choose the model structure to identify the model in continuous and later convert it into discrete. And thus, the model structure used here is Process model as described in the previous chapters, which contains a gain and a first order pole as shown in (Eq.4.16). Initially, the main idea of the identification is to match the parameters of the motor with the values contained in datasheets. But due to lack of certain information such as the model of the servo drive, the matching of parameters could not be done and the next best option was to look for the better fit model.

The fitting of the model is done in both Time domain and Frequency domain. Since it is easier to work in continuous time, the model structure was chosen to be Process model. The fit and the Bode plot for the motors Mot 37 and Mot 53 are shown in the later subsections.

Based on this, the parameters can be extracted from the model along with the frequency domain fit of the model. The frequency domain plot is produced to show the data estimation of the model, i.e., the input and output was converted in the Fast Fourier Transform (FFT). The conversion was done

with the function *fft* in MATLAB, which gives the input and output in the frequency domain and the fit of the model is found.

The parameters of the model are represented as mentioned in the (Eq. 4.16), which can be used for further use for designing of the controller. This model was further used for verification by injecting a small step and it was also verified with the Bode diagram of the system.

The Bode plot contains the transfer function using the above parameters which is in continuous time and the transfer function was also converted into Discrete time. It also contains the data estimation of the input and output in frequency domain which was done with a function *tdf* in MATLAB. This function gives the magnitudes and phases of the input and output based on different input frequencies.

The model works better with higher frequencies because the electrical time constant is too small, whereas for the lower frequencies, the estimated input and output frequencies does not even come close to the transfer function. And as the input frequency is higher, it matches well with the gain margin of the transfer function. The identification is done in time domain and later converted to frequency domain such that Bode plots show the gain margin required to maintain stability under variations in circuit characteristics caused during manufacture or during operation. And comparing the other model structures with process model structure, the identified model using process model provides a better fit, although Output error model structure came a little close as it depends on the input and output data unlike ARX model which is based on prediction of the output.

| | Inductance (mH) | Resistance (Ω) |
|---|---|---|
| Datasheet values | 1.04 | 7.03 |
| Identified Values | 2.4601 | 12.9819 |

**Table 4.1:** Motor Mot 37

| | Inductance (mH) | Resistance (Ω) |
|---|---|---|
| Datasheet values | 0.2 | 1.11 |
| Identified Values | 0.9923 | 5.1250 |

**Table 4.2:** Motor Mot 53

The Tables 4.1 and 4.2 show the difference between identified parameters and data sheet values of the motor provided by the manufacturer as shown in the Appendix A. Since the parameters of the identified model and the data sheet values does not match, the identification was done based on the fitting. And thus the following figures represents the results based on the fitting of the model.

**MOT 37:**

**Best Fit of the model**

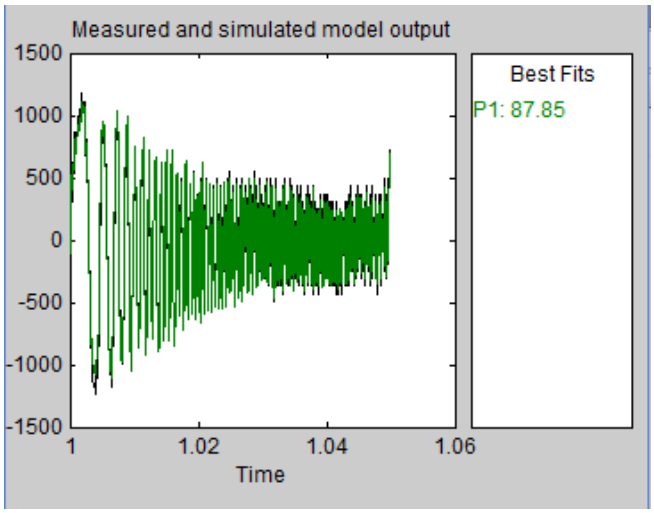


**Figure 4.8:** Fit of the electrical model in Time Domain using System Identification tool

**Bode Plot**

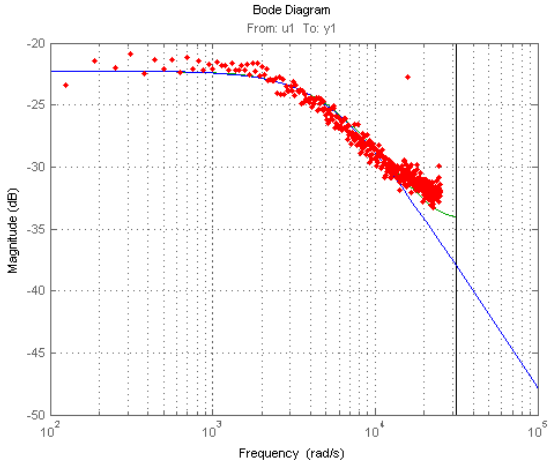


**Figure 4.9:** Bode plot of the motor MOT 37

Transfer function of the electrical part of the motor is:

$$G(s) = \frac{0.0770}{1.895e-04s+1} \tag{4.15}$$

**MOT 53:**

**Best Fit of the model**

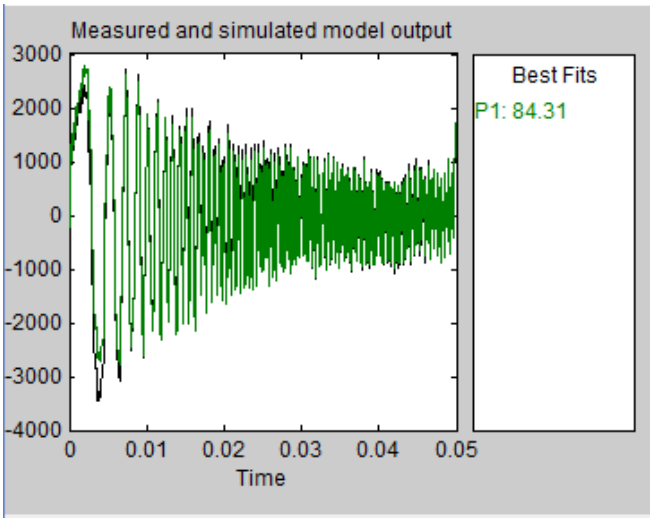


**Figure 4.10:** Fit of the electrical model in Time Domain using System Identification tool

**Bode Plot**

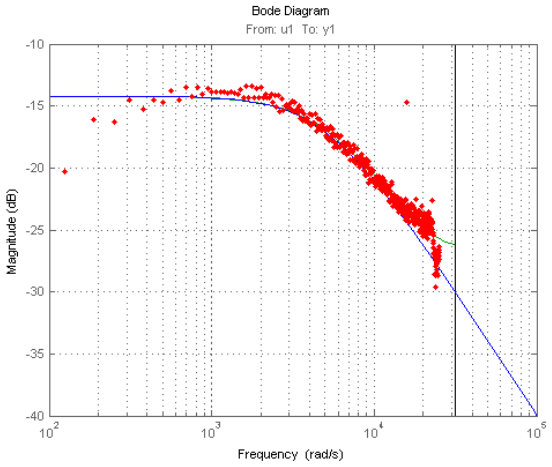


**Figure 4.11:** Bode plot of the motor MOT 53

Transfer function of the electrical part of the motor is:

$$G(s) = \frac{0.1951}{1.9363e-04s+1} \tag{4.16}$$

#### Closed loop method

There are several schemes for plant model identification in closed-loop operation including classical direct method, step identification and closed-loop output error algorithms are considered. These methods are analyzed and compared in terms of the bias distribution of the estimates for the case that the noise model is estimated as well as the case that a fixed model of noise is considered. But for the electrical characteristics, the closed-loop operation cannot be succeeded because the motor should not move as described in the previous chapters. And thus, for the closed-loop identification, the motor moves as the motor gives a step input as well as the noise, in this case, a multisinus.

#### Conclusions on the Electrical Identification

As already discussed above, the open loop identification for the electrical identification seems feasible as the closed loop identification provides information which does not identify the model of the current loop. Closed loop identification makes the system moves which allows the system identification for the position loop rather than torque loop, and thus, the closed loop identification cannot used for the identification of the electrical characteristics of the motor. For the open loop identification, the inductance and resistance does not provide the exact values of the motor provided by the manufacturer as the system might detect not only the current loop but also some effect from the outside which is very difficult to predict. But the bode plot of the open loop identification provides a better solution as the data estimated from the multisinus input matches the bode plot of the transfer function, thus making the open loop identification more effective.

### 4.3.2 Mechanical Identification

Once the file containing the values of the variables for current loop is recorded, the identification model engine starts properly. This identification will be carried out following two different methods: first, use the identification toolbox of visual character; on the other, it follows the process model method. This course of action has a dual aim: first, they can directly compare the results for each method so that you can know whether or not they are consistent; it is also a way to meet several alternatives when adjusted models.

### Identification ToolBox

The identification of MATLAB toolbox is a tool that allows for the mathematical model that best represents a data set intuitively. This operation is carried out in three stages:

**Import data:** reads the parameters previously recorded file on the MATLAB. In this case, select the option Time domain data, as the data come from a real experiment.

**Estimate:** computes the proper identification model. There are various types of estimate, according to the way they want to get the model: in the form of state space or as a transfer function as a polynomial model, etc. In this case, we opt for a process model; that is, a continuous-time transfer function that describes the dynamics of a linear system as explained in the previous chapter. This transfer function is characterized by means of a series of parameters. The selection of model and other parameters, as well as its multiplicity, the model obtained will be different in each case.

And in this case, since the current loop and position loop works on different frequency, the model of the current loop is considered to be in the position loop as a gain. But, the controller of the current loop needs to be designed before the identification of the position loop because a steady current flowing through the position loop makes the system stable. And the next thing to concentrate on how to determine the data and record them using the closed-loop techniques.

### Closed-loop method

This section deals with the identification techniques such as open loop and closed loop method and it is necessary how the techniques has been applied and which are the inputs used in this technique. As for open loop method for the mechanical identification, the motor does not move as there is no feedback for the motor output. For the identification of the mechanical model to work, the motor needs to move and this does not happen in open loop, so this technique cannot be used in the position loop.

The closed-loop method is the best way to move the motor and further determine the input and output of the model, analyse and using this data, identify the model of the motor. In this case, the method involves two inputs, namely, step input and the disturbance input for the motor as explained in the Section 4.1. This method also comes along with the proportional controller to make the motor move for the identification as shown in the figure 4.12.

The block diagram representation can further be reduced to determine the model of the motor in a easier and simpler way. The closed-loop block diagram is represented below in the figure 4.13.

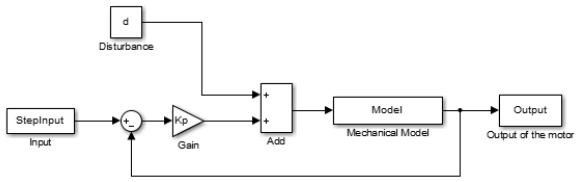


**Figure 4.12:** Closed-loop block diagram of the Mechanical model

As shown in the figure, the input is described as combination of step input and the proportional controller($Kp$) and added to the disturbance of the model as follows

$$u = StepInput * Kp + Disturbance \tag{4.17}$$

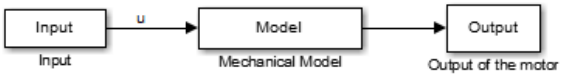


**Figure 4.13:** Reduced Closed-loop block diagram of the Mechanical model

In the MotionLab software, the reduced model was applied but the values are inserted for step input and disturbance input signal and the software automatically converts the two inputs into one. As the motor moves and the output is recorded, both input and output of the reduced model is exported into MATLAB for further analysis and the identification of the model.

Here, the output data is further reduced by removing the integrator since the identification of the model will be difficult using the current output. Thus, the derivative of the current output is used instead.

$$NewOutput(k) = \frac{Output(k) - Output(k-1)}{T_s} \tag{4.18}$$

**MOT 37:**

**Demand**

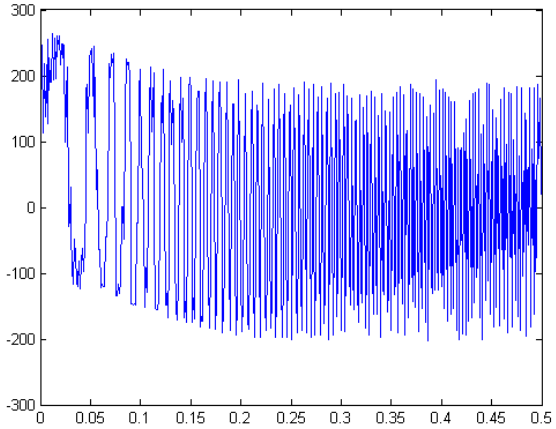


**Figure 4.14:** Input of the reduced blocked diagram represented in the Figure 4.13

**Ouptut**

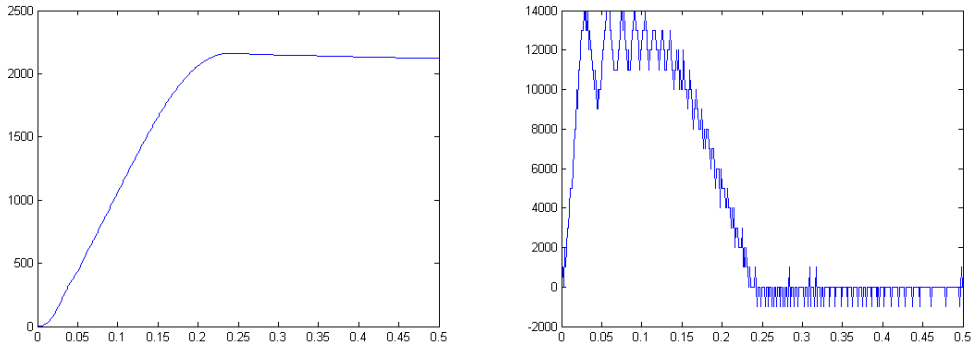


**Figure 4.15:** Position Output and Speed Output of the reduced blocked diagram represented in the Figure 4.13 respectively

**MOT 53:**

**Demand**

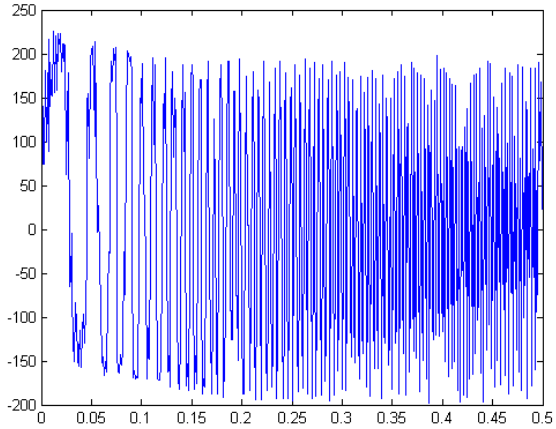


**Figure 4.16:** Input of the reduced blocked diagram represented in the Figure 4.13

**Ouptut**

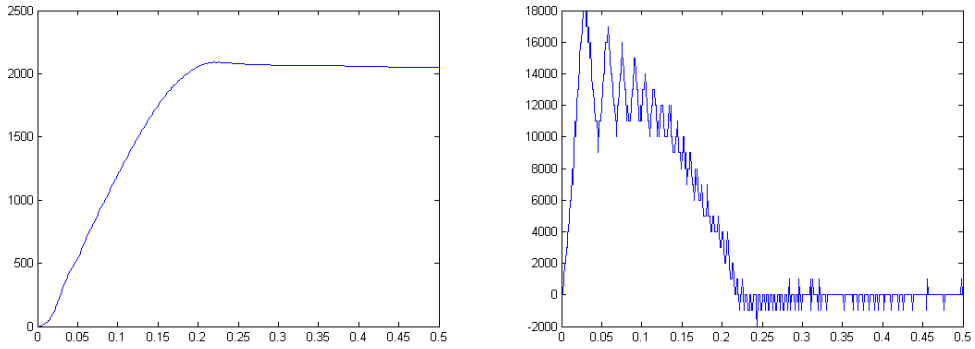


**Figure 4.17:** Position Output and Speed Output of the reduced blocked diagram represented in the Figure 4.13 respectively

This new output will be defined as a velocity output and thus the identified model will be a velocity model. The next section deals with the further analysis of data estimated using the frequency response of both the DC motors which presents various step inputs for different disturbance frequency.

**Analysis of Data estimation**

In this section, the main aim is to discuss the frequency response of the data estimated from the model from the previous subsection. The data estimated are, in general, the input and output of the system. As explained in the previous section, the input of the system is the combination of proportional controller and step input added with the disturbance as shown in the (Eq. 4.17). The output, as discussed in the previous subsection, is taken as the speed of the motor. And also, using the analysis of the data estimated, the model has been identified using the process model structure along with the results.

The main aim of this topic is to analyse the input of the reduced block diagram shown in Figure 4.13 because as the input varies, the frequency response also varies. The relation between the step input, disturbance signal and the proportional controller is the most important concept that will be dealt for the data estimation. And also, the disturbance signal can be of any frequency and in this case, the frequency injected for the disturbance signal is described as in the Section 4.1.

In the case of rotary motors, the size of the step does not have any limits on the step input. As explained in the previous Chapter 3, the step input is in counts and the input used are 2000c, 3000c and 4000c. The disturbance signal injected have a frequency of 100 Hz, 200 Hz and 400 Hz. This signal should not be injected at full amplitude as the motor will become unstable and it will be very difficult to identify the model. So, the amplitude of signal injected is approximately 10-20% as that would suffice for the identification of the mechanical model.

Now, the relation between the input and the proportional controller is very important in this case. For a higher step input, the less the proportional controller should be. As shown in the figures of the analysis shown below, there are few peaks which can be considered as the instability in the data estimation but it can be misinterpreted as the resonance.

**MOT 37:**

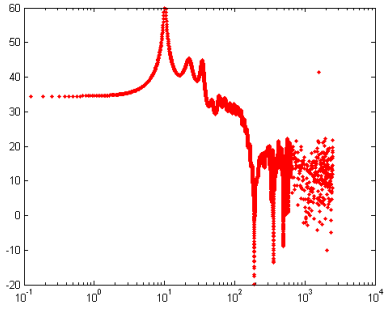

**Figure 4.18:** Data estimation for Step size = 2000c and Disturbance signal = 400 Hz with $K_p$ = 2000

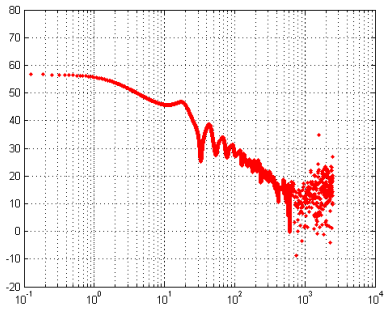

**Figure 4.19:** Data estimation for Step size = 2000c and Disturbance signal = 400 Hz with $K_p$ = 3500

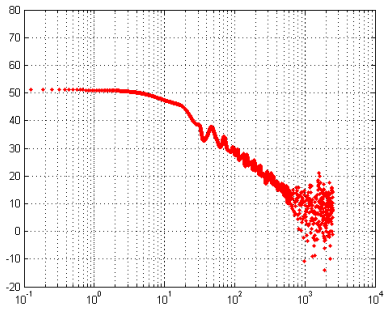

**Figure 4.20:** Data estimation for Step size = 2000c and Disturbance signal = 400 Hz with $K_p$ = 2500

**MOT 53:**

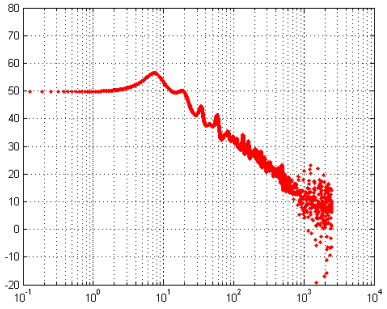

**Figure 4.21:** Data estimation for Step size = 2000c and Disturbance signal = 400 Hz with $K_p$ = 1000

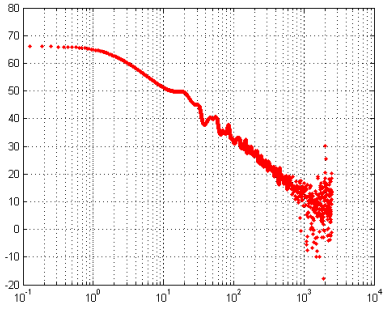

**Figure 4.22:** Data estimation for Step size = 2000c and Disturbance signal = 400 Hz with $K_p$ = 2000

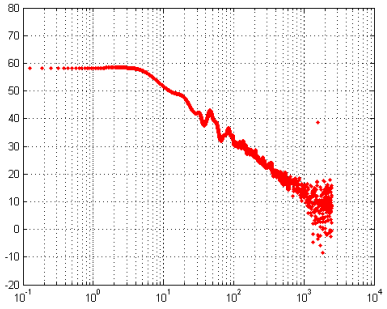

**Figure 4.23:** Data estimation for Step size = 2000c and Disturbance signal = 400 Hz with $K_p$ = 1250

From the Figures 4.18 to 4.23, it is easy to analyse that for a certain input only a particular proportional gain works which would give a stable frequency response. As seen in the Figures 4.18 and 4.21, for a lower proportional gain, the motor does not move and thus the identification will be a problem. Moreover, a peak arises due to the disturbance signal and not to the step size. Figures Freffig:data2 and 4.22 represent the unstable frequency response for the high proportional gain. As the gain increases, the motor becomes unstable and thus the frequency amplitude is higher and then becomes stable after a certain point. For a stable frequency response, the proportional gain should be properly set to match the frequency response of the data estimated to the frequency response of the model as shown in Figures 4.20 and 4.23.

The next step is to determine the model once the input and output of the model has been analysed using the above frequency response. As discussed in the Section 4.2, the process model structure is used and the first order model is to be identified as defined in the (Eq. 4.16). This model is identified as the velocity model as described in the Chapter 2 and adding an integrator block to the model gives the position loop model. The Bode diagram is plotted as shown in Figures 4.24 and 4.25. From these figures, we can say that the Process model structure have given a better fit of the velocity output of the motor and thus seems to be feasible for the verification.

As described earlier in the Section 2.2.2, the identified velocity model can be converted into position model by adding a pure integrator. In general, the parameters of the model represent three variables of a mechanical characteristics and those are

$$k = \frac{K_t}{B} \tag{4.19a}$$

$$\tau = \frac{J}{B} \tag{4.19b}$$

where $K_t$ is the torque constant which contains the gain of the current loop, $B$ is the viscous friction coefficient and $J$ is the rotor inertia.

**MOT 37:**

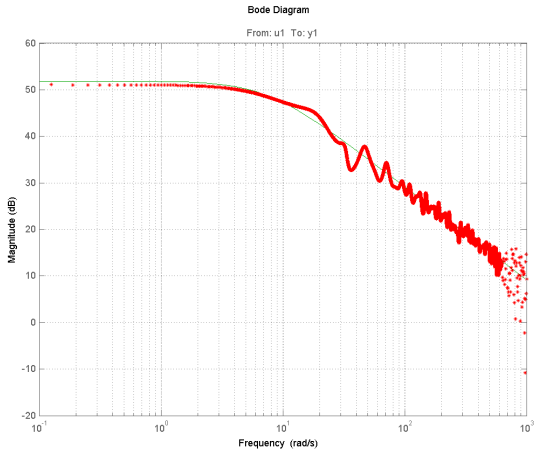


**Figure 4.24:** Bode plot of the Identified Velocity model compared with the data estimation of the model

Transfer function of the Velocity model:

$$G(s) = \frac{391.72}{0.1361s + 1} \tag{4.20}$$

Transfer function of the Position model:

$$G(s) = \frac{391.72}{s(0.1361s + 1)} \tag{4.21}$$

**MOT 53:**

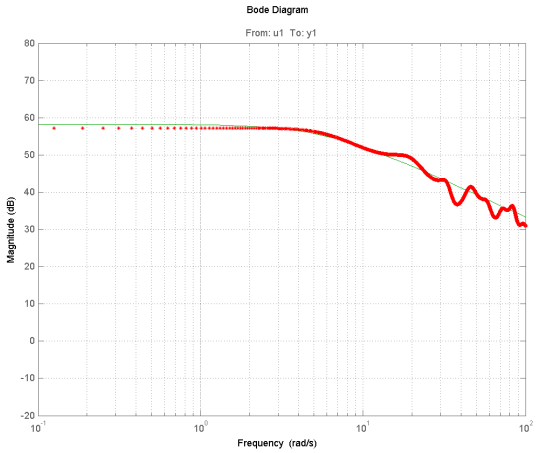


**Figure 4.25:** Bode plot of the Identified Velocity model compared with the data estimation of the model

Transfer function of the Velocity model:

$$G(s) = \frac{816.65}{0.1757s + 1} \tag{4.22}$$

Transfer function of the Position model:

$$G(s) = \frac{816.65}{s(0.1757s + 1)} \tag{4.23}$$

After the identification of the mechanical model, the next step is to verify the model of the motor. As shown in Figures 4.24 and 4.25, the frequency response of the transfer function matches the data estimated of the motor. The most important thing that needs to be taken from the Bode plot is the resonance frequency. Resonance is the tendency of a mechanical system to respond at greater amplitude when the frequency of its oscillations matches the system's natural frequency of vibration than it does in other frequencies. For the motor MOT 37, the resonance frequency is 5.1 Hz and for the motor MOT 53, the resonance frequency is 5.5 Hz.

**Conclusions on the Mechanical Identification**

As seen from the figures of the Bode plot and the analysis of data estimation, we can conclude by saying that the process model structure seems to have so much effect in the system than the ARX or OE model structures. And also, the original position output was further reduced as the identification of the position loop seems to be a little complicated as it was imported in the MATLAB in the system identification application. Thus, the position output was reduced to velocity output by removing the integrator using a linear extrapolation technique as described in the (Eq. 4.18).

The resonance of the Bode plot can be solved using a controller. The next chapter deals with the designing of the controllers for both electrical characteristics and the mechanical characteristics of the motor. And the verification of the model can be done in the SIMULINK using the PID controllers that will be discussed in the next chapter.

# Chapter 5

# Design of Controllers

The main aim of this chapter is to design the controller and solve the resonance in the mechanical system of the motor. The controller is designed using the pole placement technique approach as described in [5] and combining the concept as presented in the Section 2.3. This chapter is structures is as follows: firstly, designing controller for current loop, secondly, designing of PID controller for position loop and the final section deals with comparison of the simulation with the real world.

Pole placement method is a controller design method in which the closed loop poles on the complex plane are fixed. Poles describe the behaviour of linear dynamical systems. Through use of feedback, the behaviour can be changed in a way that is more favourable for stabilising the model. The closed loop poles can be placed at a certain point and force them to be there by designing a feedback control system via pole placement method where the controller gains can be predicted.

## 5.1 Current Loop

In this section, the important topic is to discuss the designing of the PI controller for the electric model of the motor using pole placement technique. As described in the control law in the Chapter 2, the electrical model can be controlled using the PI controller. The controller involves the proportional gain and integral gain which stabilises the model.

For designing the controller, the transfer function of the closed loop model needs to be determined. This is shown in the (Eq. 5.1) that is derived from the Figure 5.1.

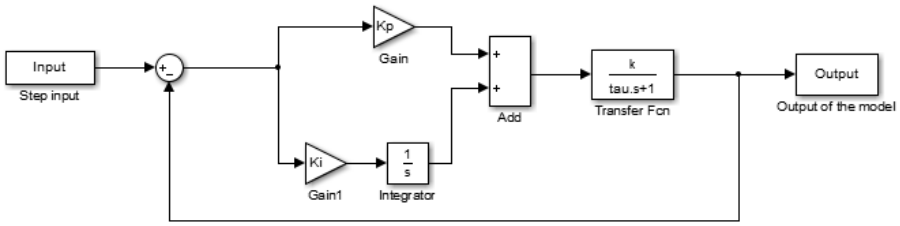


**Figure 5.1:** Closed loop Electrical model block diagram along with the PI controller

$$H(s) = \frac{(K_p s + K_i)k}{s(\tau s + 1) + K_p k s + K_i k} \tag{5.1}$$

The PI controller can be designed using the electrical model which is described in the (Eq. 4.16). Thus, the poles of the model can be placed at s = $\frac{-1}{\tau}$. In this case, the poles of the model can be placed as two points on the pole-zero plot and using the values of $k$ and $\tau$, the values of $K_p$ and $K_i$ can be obtained as follows

$$\begin{aligned} s(\tau s + 1) + K_p k s + K_i k &= (s + \frac{1}{\tau})^2 \\ &= (s + pol)^2 \end{aligned} \tag{5.2}$$

From the above (Eq. 5.2), we get the controller gains in the form of,

$$K_p = \frac{2pol\tau - 1}{k} \tag{5.3a}$$

$$K_i = \frac{pol^2\tau}{k} \tag{5.3b}$$

After the designing of controller for the electrical model, the next step is to verify the model with the real world environment, using the MotionLab software. As seen from the Figures 5.2 and 5.3, there are few quantization error in the current loop because of the current resolution range. And we can conclude that the PI controller has been designed for better system performance.

**MOT 37:**

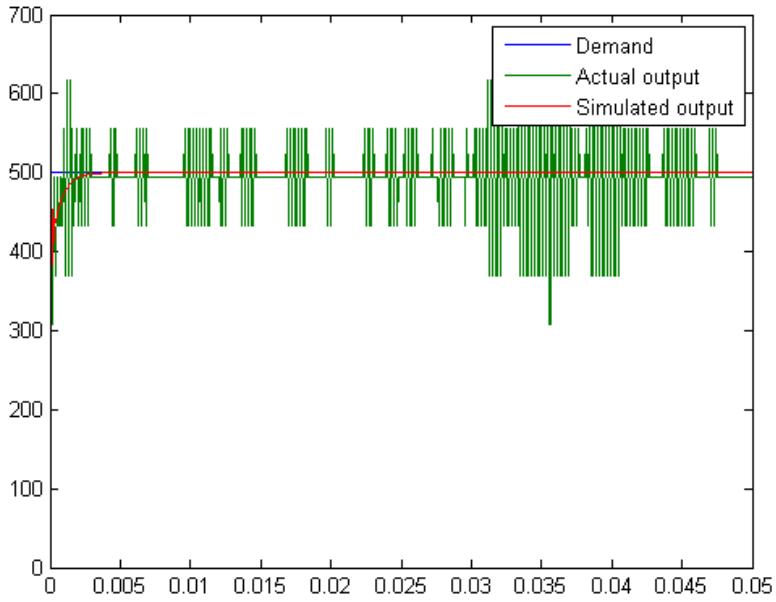


**Figure 5.2:** PI controller design verification of the model compared with real world

$$K_p = 38.9458; K_i = 6.8505e + 4;$$

**MOT 53:**

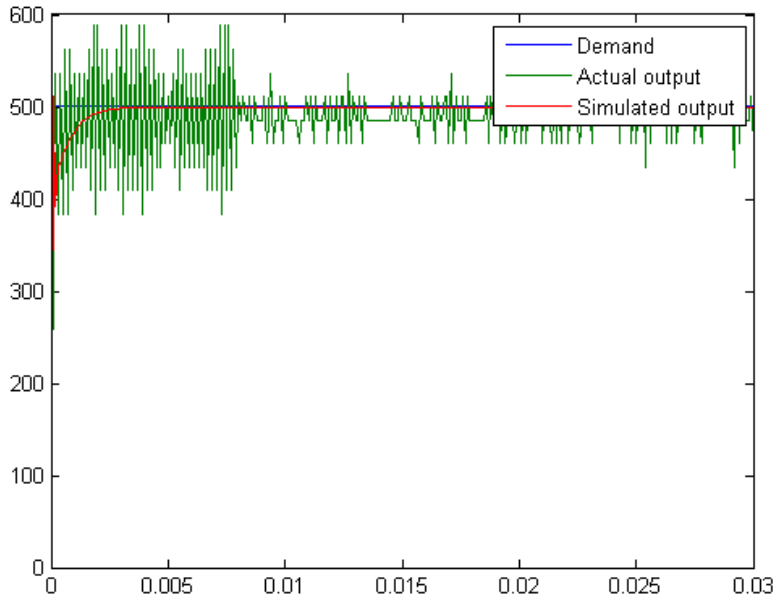


**Figure 5.3:** PI controller design verification of the model compared with real world

$$K_p = 15.3748; K_i = 2.6468e + 4;$$

## 5.2 Position loop

After the designing of the electrical model, the next step is determine the controller gains that are again calculated using the pole placement technique. As described in the Section 2.3, the controller design contains three unknown variables $K_p$, $K_i$ and $K_d$ which are defined as proportional gain, integral gain and derivative gain respectively.

As previously discussed, the PID controller can be calculated using poles of the closed loop model by determining the transfer function of the closed loop block diagram as shown in the Figure 5.4. The transfer function of the closed loop transfer function can be defined as represented in the following

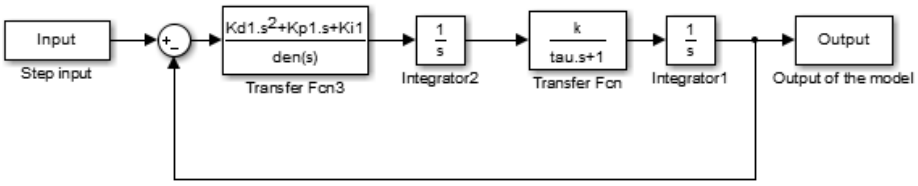


**Figure 5.4:** Closed loop Mechanical model block diagram along with the PID controller

$$H(s) = \frac{(K_d s^2 + K_p s + K_i)k}{\tau s^3 + (1 + K_d k)s^2 + K_p k s + K_i k} \tag{5.4}$$

The PID controller can be designed using the mechanical model which is described in the (Eq. 4.7). Thus, the poles of the model can be placed at s = $\frac{-1}{\tau}$. In this case, the poles of the model can be placed at three points on the pole-zero plot and using the values of k and $\tau$, the values of $K_p$, $K_i$ and $K_d$ can be obtained as shown in the following

$$\begin{aligned} \tau s^3 + (1 + K_d k)s^2 + K_p k s + K_i k &= (s + \frac{1}{\tau})^3 \\ &= (s + pol)^3 \end{aligned} \tag{5.5}$$

$$K_p = \frac{3\tau pol^2}{k} \tag{5.6a}$$

$$K_i = -\frac{\tau pol^3}{k} \tag{5.6b}$$

$$K_d = \frac{-3\tau pol - 1}{k} \tag{5.6c}$$

The values of the $K_p$, $K_i$ and $K_d$ are given below and using these values, the verification can be done in the real world and in simulation. The main problem, in this case, arises in the simulation as there is an overshoot in the model as shown in Figures 5.6 and 5.8. To avoid the overshoot in the model, the best way is to solve the problem using the I-PD controller where the proportional and the derivative are added as a feedback and the integral will be in series as shown in the Figure 5.5.

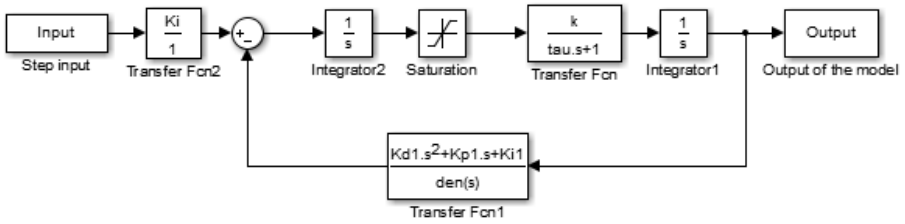


**Figure 5.5:** Closed loop Mechanical model block diagram along with the I-PD controller

$$H(s) = \frac{K_i k}{\tau s^3 + (1 + K_d k)s^2 + K_p k s + K_i k} \tag{5.7}$$

From the (Eq. 5.7), the denominator seems to be the same as for the PID controller but the most important thing is the numerator. For a PID controller, the numerator has a second order laplace transform whereas for I-PD controller, the numerator has a gain alone. And this might be the reason behind the overshoot in the PID controller as the numerator seems to have some effect in the system. The results of the I-PD controller is represented in the Figures 5.7 and 5.9 and the values of the PID controller is represented below for both the motors.

**MOT 37:**

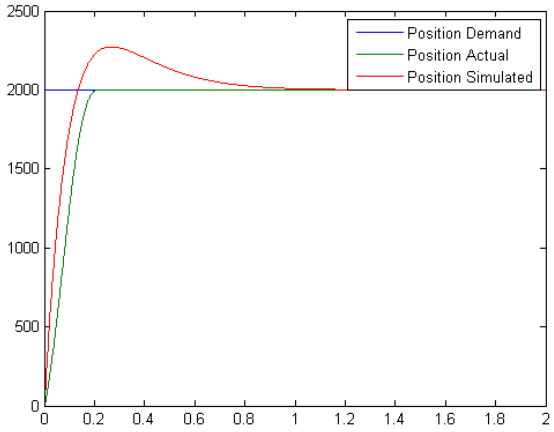


**Figure 5.6:** PID controller design verification of the model compared with real world

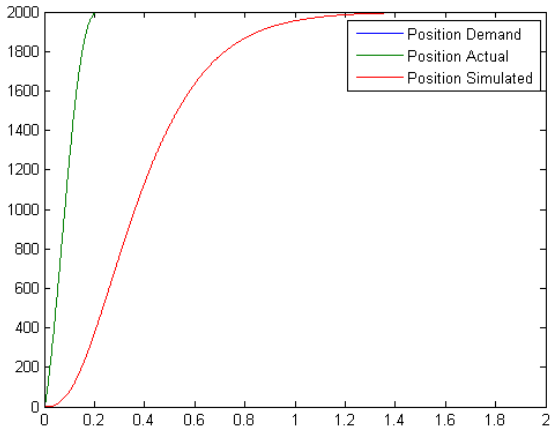


**Figure 5.7:** IPD controller design verification of the model compared with real world

$$K_p = 0.0562; K_i = 0.1377; K_d = 0.0051;$$

**MOT 53:**

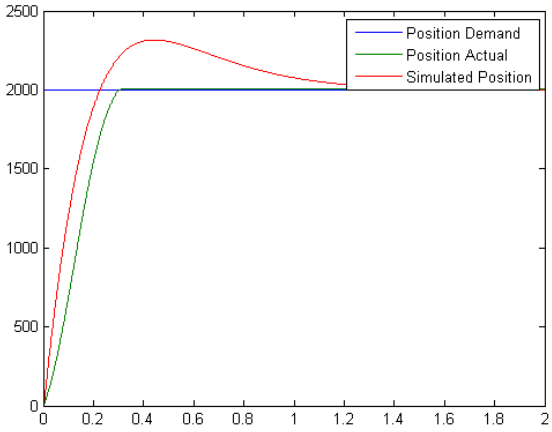


**Figure 5.8:** PID controller design verification of the model compared with real world

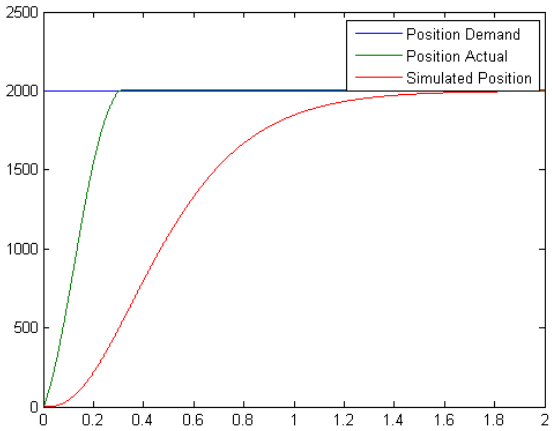


**Figure 5.9:** IPD controller design verification of the model compared with real world

$$K_p = 0.0209; K_i = 0.0396; K_d = 0.0024;$$

**Conclusions on the Control Design**

First, to summarize, the controller has been designed in continuous time as the model identified is in continuous time. Keeping in mind, however, that the current programs Ingenia version only allows to implement PID controller. However, the suggestion is to develop different control schemes to provide feasible results based on the results obtained above. The original presents continuous PID controller with an overshoot, which corrects the I-PD controller continuum - slightly modified. Another important conclusion, the designing of the controller was done using the pole placement technique rather than using the bandwidth to design the controller as depicted in the Section 2.3.2.

# Chapter 6

# Environment impact study

The application of the method presented in this paper for the identification and control of DC motors, will have more impact on economic rather than environmental, but can perform some actions to minimize the effects of the project may cause to the environment. Developing codes for tuning controllers provide constant driver directly based on the specification in the system bandwidth, reduces the calculation time of the control problem. It is expected that the savings in time have a positive economic impact.

The environmental impact of this project will be small as energy consumption mainly needed to power the motor - is very low, and the life of your motor is sufficiently long as not to become a problem. However, this impact can be reduced if the motors are recycled properly at the end of its useful life: you can dismantle and classify expensive components in terms of materials, recover the valuable materials that can still do service. It does not generate any toxic residue, smoke, etc., necessary to treat. That is why the environmental impact of the project will be minimal.

# Chapter 7

# Conclusions

This chapter is not intended to repeat the analysis of the results of identification and control, which has already made the final of each of the respective chapters. Instead, its goal is to give general guidelines based on experience gained during the implementation of this project. Regarding the identification of system, it is interesting to analyse the data estimation, especially the input of the model. Clearly, the identification of the system depends on the input and the feedback of the encoder as it is difficult to predict the proportional gain using the trial and error method. And also noticed is the fact that the identification works better with continuous-time system than the discrete time.

Another interesting factor in this project is to eliminate the effect of integrators in the data provided that their presence known before: it has been verified that this substantially improves the results of the adjustment of the models. It is recalled that it was necessary to perform this procedure for motor Ingenia because it had no speed sensor, and thus the appearance of a pure integrator gives the measure of position output. With regard to control, it is interesting to note that the improvement in motor response is obtained by passing the original PID structure alternatives I-PD because of the overshoot.

In the near future, we will be concentrating on shaping the sensitivity function for the input of the plant model. In this case, we will be shaping the sensitivity input function to control the peak movement of the motor according to the saturation point. And also, we explore the frequency domain techniques for design of the feedback model systems. Initially, it is based on identied continuous-time systems of the motor involving the PID controller designed using the pole placement method combined with sensitivity function in the frequency domain. In this case, the maximum peak has to

be determined and using the knowledge from the paper [6]. From this paper, we determine the upper template of the model and also the sensitivity function and applying a condition where the norm of the product of upper template and the input sensitivity function should be less the amplitude of the saturation limit. This will control the input of the plant model and gives the maximum limit as shown in Figure 7.1.

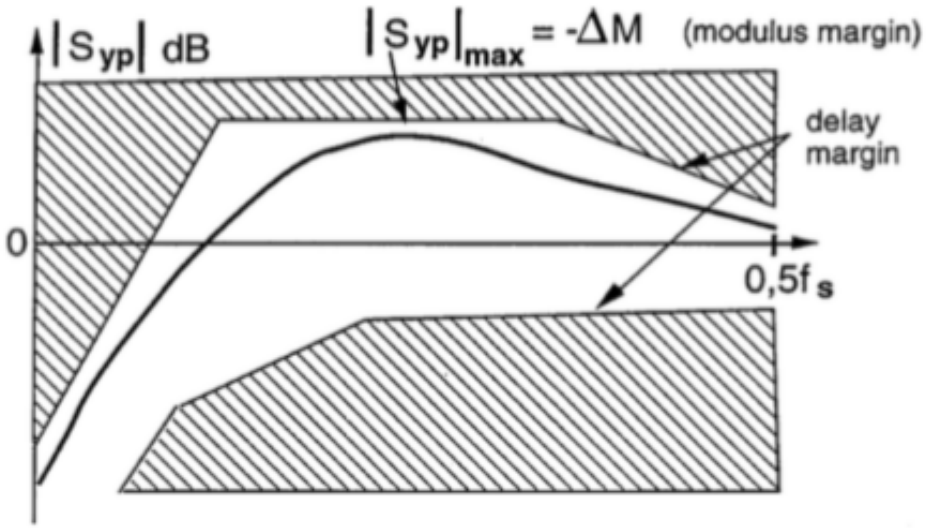


**Figure 7.1:** Desired template for the input sensitivity function

Also, for the future, we will be interested in trying to improve the problems found while implementing a basic PID control scheme related to frictions and delays in the loop. Basically, the dynamic model is linear in the state and control variables. However, a non-linearity is present because of modelling the static coulomb friction and is modelled via a jump function depending on the sign of the velocity. This leads to a non-smooth optimal control problem and the system becomes a non-linear control system. We will deal with the non-linearity and involving the study of the non-linear concepts and the compensation of the non-linear eects in the system.

# Chapter 8

# Cost of the project

In this chapter, the time invested, the assets used and various expenses will be discussed that have been necessary for the development of this project.

The budget of this project is considered to be as follows:

| Concept | Cost [€] |
|---|---|
| Maxon 253447 Motor Mot 37 | 290.00 |
| Maxon 199809 Motor Mot 53 | 290.00 |
| Pluto DC Servo drive | 600.00 |
| DC power supply (24V) | 145.00 |
| Software license Matlab® | 2000.00 |
| Software license Simulink® | 3000.00 |
| Assets cost | 6325.00 |
| Miscellaneous expenses | 250.00 |
| SubTotal | 6575.00 |
| Overhead costs (5%) | 328.75 |
| Salary | 13750.00 |
| Total cost | 20,653.75 |

The table above gives the overall budget implementation of the project that was used for its development. The first part of the table contains all the assets used in this whole project that have been discussed in the Chapter 3.

Miscellaneous expenses includes, travel expenses, energy used, paper, food, etc., which is approximately estimated during the project.

As for salary, it can be split into two parts, one for the project manager and the other for the student. It is estimated that the project manager, who is assigned a salary of 50e / hour, has devoted about 70 hours to the project, and in this case, two project managers were assigned, thus the salary doubles; the student contemplates a salary of 15e / hour and 450 hours of total dedication to the project.

## Acknowledgements

I want to thank to my supervisor *Vicenç Puig* for guiding me and teaching me along this thesis. And I also want to thank my advisors from the company *Roger Juanpere* and *Rob Verhaart* for helping me provide their workspace for this thesis. I am very grateful for all your help and allow me to learn so much.

A big thanks to my family, especially my mother for always supported me during all these years and for allowing me to study these two years in Barcelona and undertake this journey and also shared my pains and my joys during this run

And of course to all my roommates and friends, who helped me in motivating myself and helping me throughout the semester.

# Chapter 9

# Bibliography


[1] Mathworks. http://in.mathworks.com/help/ident/ug/what-is-a-process-model.html.

[2] Mathworks. http://in.mathworks.com/help/ident/ug/what-are-polynomial-models.html?searchHighlight=polynomial%20model%20structure.

[3] Pablo Segovia Castillo. Vicenç Puig Cayuela. Identificació i control d'un motor de tipus voice coil. 2014.

[4] Karel J. Keesman. System identification techniques. In *System Identification*, volume 2.

[5] I. Landau and G. Zito. Digital control systems: Design, identication and implementation. 2006.

[6] I.D. LANDAU* and A. KARIMI. Robust digital control using pole placement with sensitivity function shaping method. 1998.

[7] Lennart Ljung. Model structure selection and model validation. In *System Identification: Theory for the User, Second Edition*, volume 16, pages 408–431. Linkoping University Sweden.

[8] Lennart Ljung. Practical issues of system identification, choice of signals. http://www.eolss.net/EolssSampleChapters/C05/E6-43-12/E6-43-12-TXT-03.aspx.

[9] Luca Zaccarian. *DC motors: dynamic model and control techniques*, chapter 2.

# Appendix A

# Matlab codes and Datasheet of Motors

```
clear all
clc

%\% Electrical Identification Testing
% Mutisine 20:20:4000
f = fullfile('Torque','Output','Multisine20.csv');
load(f);
t = Multisine20(:,1); t = t/10000;
T_actual = Multisine20(:,2);
T_demand = Multisine20(:,3);

Ts = 1/10000;

% Transfer function identified model

load('P1_M50.mat');

% Gz = tf(oe111.B,oe111.F,Ts);
G = tf(P1); % d2c(Gz);
[num,den] = tfdata(G,'v');
Gz = c2d(G,Ts);

k = num(2); tau = den(1);
R = 1/k
L = tau*R
```

```
%% PI controller design
syms Kp1 Ki1 s;
p = pole(G);
C1 = (s^2)+((1+Kp1*k)/tau)*s+(k*Ki1/tau);
C2 = (s + p)^2;

S = coeffs(C1-C2,s);

Kp1 = -double(solve(S(2),Kp1))
Ki1 = double(solve(S(1),Ki1))
% Ki1 = (1/a)*(2*p-d-b*Kp1);
% Kp1 = (1/b)*(2*p-d-a*Ki1);

Kp = Kp1*(2^15)/(2^6)
Ki = Ki1*(2^15)*Ts/(2^6)

C = tf([Kp1 Ki1],[1 0]);

sys = feedback(C*G,1);
```

**Listing A.1:** Identification and control of Current loop

```
clear all;
clc

%% Mechanical identification with velocity output
f = fullfile('Position','Output','Multisine4000','Multisine2000_1.csv');
load(f);
t = Multisine2000_1(:,1); t = t/1000; tmax = max(t);
P_actual = Multisine2000_1(:,2);
P_demand = Multisine2000_1(:,3);

Ts = 1/1000;

y = zeros(length(P_actual), 1);

y(1) = P_actual(1);
k = 2;
```

```
17
while (k<501)
19      y(k) = (P_actual(k)-P_actual(k-1))/(1*Ts); %dona y(k)*Ts degut a l'aproximacio
        k = k+1;
21  end

23  %% Transfer function deduction

25  f = fullfile('Position','Output','Multisine4000','P2000.mat');
    load(f);
27

    Gmotor = tf(P1);
29  [num,den] = tfdata(P1,'v');
    k = num(2); tau = den(1);
```

**Listing A.2:** Identification of Position Loop

```
1   clear all;
    clc
3

    %% Mechanical identification with velocity output
5   f = fullfile('Position','Output','Multisine4000','Multisine2000_3.csv');
    load(f);
7   t = Multisine2000_3(:,1); t = t/1000;
    P_actual = Multisine2000_3(:,2);
9   P_demand = Multisine2000_3(:,3);

11  Ts = 1/1000;

13  y = zeros(length(P_actual), 1);

15  y(1) = P_actual(1);
    k = 3;
17

    while (k<501)
19      y(k) = (P_actual(k)-P_actual(k-1))/(1*Ts);
        k = k+1;
21  end
```

```
%% Transfer function deduction

f = fullfile('Position','Output','Multisine4000','P2000.mat');
load(f);

Gmotor = tf(P1);
[num,den] = tfdata(P1,'v');

%% Bode
f1 = 0:0.01:100;
f2 = 101:1:400;
fr = [f1 f2];
wr = 2*pi*fr;
Fs = 1000;
Ts = 1/Fs;

[gu, fu] = tdf(P_demand, fr, Ts, 0);
[ga, fa] = tdf(P_actual, fr, Ts, 0);
[gy, fy] = tdf(y, fr, Ts, 0);


figure(1)
title('Frequency Response of Motor');
bodemag(Gmotor,'g')
grid on
hold on
% bodemag(Gmotor,'b')
% bodemag(Cmotor,'b')
% bodemag(sysMotor,'m')
semilogx(wr, 20*log10(gy./gu),'r*','MarkerSize',3)
xlim([-0.1 100000]); ylim([-20 60]);
% file_pic = fullfile('Pics','Multisine1000','P4000','Multisine4000_3.png');
% saveas(gcf,file_pic);
```

**Listing A.3:** Data estimation of Position Loop

```
clear all;
clc

%% Mechanical identification 5% amplitude noise on step
f = fullfile('Position','Output','SamplePID2.csv');
load(f);
t = SamplePID2(:,1); t = t/1000; tmax = max(t);
P_actual = SamplePID2(:,2);
P_demand = SamplePID2(:,3);

Ts = 1/1000;

y = zeros(length(P_actual), 1);

y(1) = P_actual(1);
k = 2;

while (k<501)
    y(k) = (P_actual(k)-P_actual(k-1))/(1*Ts); %dona y(k)*Ts degut a l'aproximacio
    k = k+1;
end

%% Transfer function deduction

f = fullfile('Position','Output','Multisine4000','P2000.mat');
load(f);

Gmotor = tf(P1);
[num,den] = tfdata(P1,'v');
k = num(2); tau = den(1);

%% Controller design
pol = -pole(Gmotor); Ks = 65536;
Kd1 = (3*pol*tau-1)/k;
Kp1 = (3*(pol^2)*tau)/k;
Ki1 = (((pol)^3)*tau)/k;

```

```
Kp = Kp1*Ks
Ki = Ki1*(Ks*Ts)
Kd = Kd1*(Ks/Ts)

y1 = [t y];
Demand_in = [t P_demand];
Actual = [t P_actual];
sim('Verification');

figure
plot(Demand.time,Demand.Data,Real.time,Real.Data,Position.time,Position.Data);
legend('Position Demand','Position Actual','Position Simulated');

figure
plot(Demand.time,Demand.Data,Real.time,Real.Data,PositionMotionLab.time,PositionMotionLab.
    Data);
legend('Position Demand','Position Actual','Position Simulated');
% file_pic = fullfile('Pics','SamplePID.png');
% saveas(gcf,file_pic);

% figure
% plot(y.time,y.Data,Velocity.time,Velocity.Data);
% legend('Velocity actual','Velocity simulated');
```

**Listing A.4:** Control of Position Loop

# A-max 32 ∅32 mm, Graphite Brushes, 15 Watt

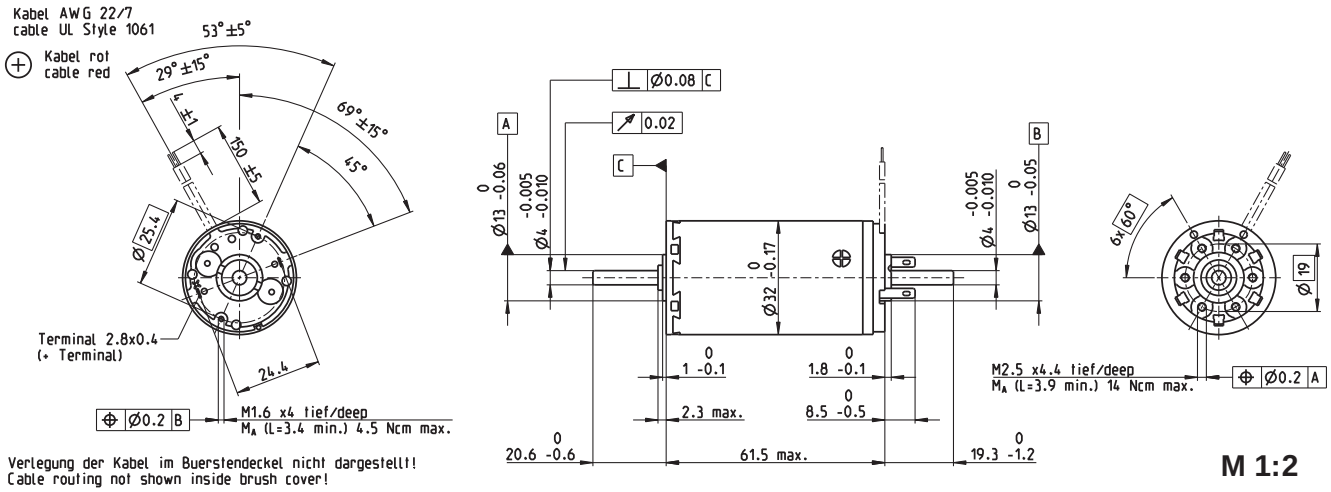


Stock program
Standard program
Special program (on request)

## Part Numbers

| | | | | | | | | |
|---|---|---|---|---|---|---|---|---|
| with terminals | 236651 | 236652 | **236653** | 236654 | **236655** | 236656 | 236657 | 236658 |
| with cables | 353220 | 353221 | 353222 | 353223 | 353224 | 353225 | 353226 | 353227 |

## Motor Data

| | | | | | | | | | |
|---|---|---|---|---|---|---|---|---|---|
| | **Values at nominal voltage** | | | | | | | | |
| 1 | Nominal voltage | V | 6 | 9 | 12 | 18 | 24 | 30 | 36 | 48 |
| 2 | No load speed | rpm | 5870 | 4940 | 4680 | 5280 | 5930 | 5870 | 5830 | 3870 |
| 3 | No load current | mA | 154 | 83.5 | 58.6 | 44.9 | 38.7 | 30.6 | 25.3 | 11.8 |
| 4 | Nominal speed | rpm | 4110 | 3090 | 2920 | 3590 | 4210 | 4160 | 4100 | 2090 |
| 5 | Nominal torque (max. continuous torque) | mNm | 36.5 | 35 | 37.2 | 38.3 | 37.3 | 37.5 | 37.1 | 37 |
| 6 | Nominal current (max. continuous current) | A | 3.95 | 2.12 | 1.6 | 1.23 | 1.01 | 0.806 | 0.66 | 0.328 |
| 7 | Stall torque | mNm | 127 | 95.3 | 101 | 122 | 130 | 130 | 127 | 81.6 |
| 8 | Stall current | A | 13.2 | 5.58 | 4.19 | 3.78 | 3.42 | 2.7 | 2.17 | 0.7 |
| 9 | Max. efficiency | % | 78 | 76 | 77 | 79 | 80 | 80 | 80 | 76 |
| | **Characteristics** | | | | | | | | |
| 10 | Terminal resistance | Ω | 0.454 | 1.61 | 2.86 | 4.76 | 7.03 | 11.1 | 16.6 | 68.6 |
| 11 | Terminal inductance | mH | 0.066 | 0.209 | 0.416 | 0.739 | 1.04 | 1.66 | 2.43 | 9.71 |
| 12 | Torque constant | mNm/A | 9.58 | 17.1 | 24.1 | 32.2 | 38.2 | 48.2 | 58.3 | 117 |
| 13 | Speed constant | rpm/V | 996 | 559 | 396 | 297 | 250 | 198 | 164 | 81.9 |
| 14 | Speed / torque gradient | rpm/mNm | 47.2 | 52.8 | 47 | 44 | 46 | 45.6 | 46.6 | 48.2 |
| 15 | Mechanical time constant | ms | 21.9 | 21.7 | 21.4 | 21.3 | 21.3 | 21.3 | 21.4 | 21.5 |
| 16 | Rotor inertia | gcm² | 44.2 | 39.2 | 43.5 | 46.2 | 44.2 | 44.6 | 43.8 | 42.6 |

## Specifications

| | | |
|---|---|---|
| | **Thermal data** | |
| 17 | Thermal resistance housing-ambient | 7.5 K/W |
| 18 | Thermal resistance winding-housing | 2.1 K/W |
| 19 | Thermal time constant winding | 17.8 s |
| 20 | Thermal time constant motor | 791 s |
| 21 | Ambient temperature | -20…+85°C |
| 22 | Max. winding temperature | +125°C |
| | **Mechanical data (ball bearings)** | |
| 23 | Max. speed | 6000 rpm |
| 24 | Axial play | 0.12 - 0.22 mm |
| 25 | Radial play | 0.025 mm |
| 26 | Max. axial load (dynamic) | 7.6 N |
| 27 | Max. force for press fits (static) | 110 N |
| | (static, shaft supported) | 2000 N |
| 28 | Max. radial load, 5 mm from flange | 32 N |
| | **Mechanical data (sleeve bearings)** | |
| 23 | Max. speed | 6000 rpm |
| 24 | Axial play | 0.12 - 0.22 mm |
| 25 | Radial play | 0.012 mm |
| 26 | Max. axial load (dynamic) | 5.0 N |
| 27 | Max. force for press fits (static) | 110 N |
| | (static, shaft supported) | 2000 N |
| 28 | Max. radial load, 5 mm from flange | 10.5 N |
| | **Other specifications** | |
| 29 | Number of pole pairs | 1 |
| 30 | Number of commutator segments | 13 |
| 31 | Weight of motor | 210 g |

Values listed in the table are nominal.
Explanation of the figures on page 107.

**Option**
Sleeve bearings in place of ball bearings

## Operating Range

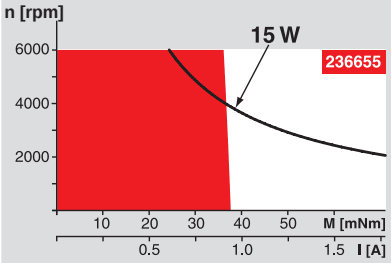


## Comments

**Continuous operation**
In observation of above listed thermal resistance (lines 17 and 18) the maximum permissible winding temperature will be reached during continuous operation at 25°C ambient.
= Thermal limit.

**Short term operation**
The motor may be briefly overloaded (recurring).

**Assigned power rating**

## maxon Modular System

Overview on page 20–25

**Planetary Gearhead**
∅32 mm
0.75 - 6.0 Nm
Page 303–308

**Spur Gearhead**
∅38 mm
0.1 - 0.6 Nm
Page 313

**Spindle Drive**
∅32 mm
Page 334–336

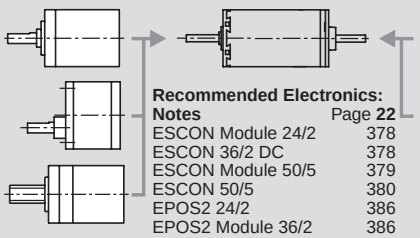

**Recommended Electronics:**

| Notes | Page 22 |
|---|---|
| ESCON Module 24/2 | 378 |
| ESCON 36/2 DC | 378 |
| ESCON Module 50/5 | 379 |
| ESCON 50/5 | 380 |
| EPOS2 24/2 | 386 |
| EPOS2 Module 36/2 | 386 |
| EPOS2 24/5, EPOS2 50/5 | 387 |
| EPOS2 P 24/5 | 390 |
| EPOS3 70/10 EtherCAT | 393 |
| MAXPOS 50/5 | 396 |

**Encoder MR**
256 - 1024 CPT,
3 channels
Page 356

**Encoder HED_ 5540**
500 CPT,
3 channels
Page 363/365

# Encoder HEDS 5540 500 CPT, 3 Channels

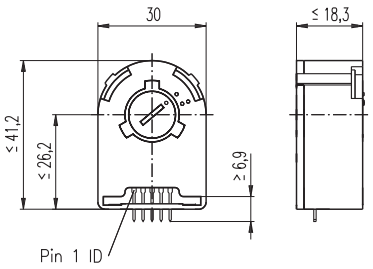


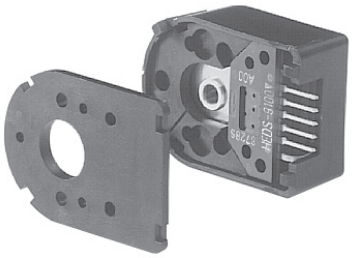

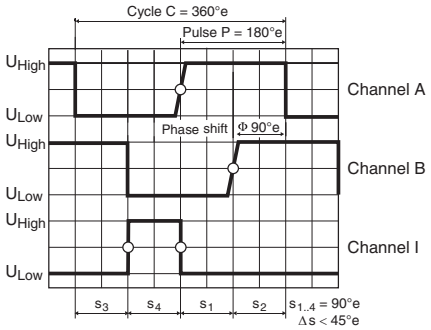


Direction of rotation cw (definition cw p. 106)

Stock program
Standard program
Special program (on request)

| Part Numbers | 110511 | 110513 | 110515 |
|---|---|---|---|
| **Type** | | | |
| Counts per turn | 500 | 500 | 500 |
| Number of channels | 3 | 3 | 3 |
| Max. operating frequency (kHz) | 100 | 100 | 100 |
| Max. speed (rpm) | 12000 | 12000 | 12000 |
| Shaft diameter (mm) | 3 | 4 | 6 |


## maxon Modular System

| + Motor | Page | + Gearhead | Page | + Brake | Page | Overall length [mm] / ● see Gearhead | | | | | |
|---|---|---|---|---|---|---|---|---|---|---|---|
| RE 25 | 135/137 | | | | | 75.3 | | | | | |
| RE 25 | 135/137 | GP 26, 0.75 - 2.0 Nm | 301 | | | ● | | | | | |
| RE 25 | 135/137 | GP 32, 0.75 - 6.0 Nm | 303-307 | | | ● | | | | | |
| RE 25 | 135/137 | KD 32, 1.0 - 4.5 Nm | 312 | | | ● | | | | | |
| RE 25 | 135/137 | GP 32 S | 334-336 | | | ● | | | | | |
| RE 25, 20 W | 137 | | | AB 28 | 408 | 105.8 | | | | | |
| RE 25, 20 W | 137 | GP 26, 0.75 - 2.0 Nm | 301 | AB 28 | 408 | ● | | | | | |
| RE 25, 20 W | 137 | GP 32, 0.75 - 6.0 Nm | 303-307 | AB 28 | 408 | ● | | | | | |
| RE 25, 20 W | 137 | KD 32, 1.0 - 4.5 Nm | 312 | AB 28 | 408 | ● | | | | | |
| RE 25, 20 W | 137 | GP 32 S | 334-336 | AB 28 | 408 | ● | | | | | |
| RE 30, 15 W | 138 | | | | | 88.8 | | | | | |
| RE 30, 15 W | 138 | GP 32, 0.75 - 4.5 Nm | 305 | | | ● | | | | | |
| RE 30, 60 W | 139 | | | | | 88.8 | | | | | |
| RE 30, 60 W | 139 | GP 32, 0.75 - 6.0 Nm | 303-309 | | | ● | | | | | |
| RE 30, 60 W | 139 | KD 32, 1.0 - 4.5 Nm | 312 | | | ● | | | | | |
| RE 30, 60 W | 139 | GP 32 S | 334-336 | | | ● | | | | | |
| RE 35, 90 W | 140 | | | | | | 91.7 | | | | |
| RE 35, 90 W | 140 | GP 32, 0.75 - 8.0 Nm | 303-310 | | | | ● | | | | |
| RE 35, 90 W | 140 | GP 42, 3.0 - 15 Nm | 314 | | | | ● | | | | |
| RE 35, 90 W | 140 | GP 32 S | 334-336 | | | | ● | | | | |
| RE 35, 90 W | 140 | | | AB 28 | 408 | 124.3 | | | | | |
| RE 35, 90 W | 140 | GP 32, 0.75 - 8.0 Nm | 303-310 | AB 28 | 408 | ● | | | | | |
| RE 35, 90 W | 140 | GP 42, 3.0 - 15 Nm | 314 | AB 28 | 408 | ● | | | | | |
| RE 35, 90 W | 140 | GP 32 S | 334-336 | AB 28 | 408 | ● | | | | | |
| RE 40, 25 W | 141 | | | | | 91.7 | | | | | |
| RE 40, 150 W | 142 | | | | | | 91.7 | | | | |
| RE 40, 150 W | 142 | GP 42, 3.0 - 15 Nm | 314 | | | | ● | | | | |
| RE 40, 150 W | 142 | GP 52, 4.0 - 30 Nm | 318 | | | | ● | | | | |
| RE 40, 150 W | 142 | | | AB 28 | 408 | 124.3 | | | | | |
| RE 40, 150 W | 142 | GP 42, 3.0 - 15 Nm | 314 | AB 28 | 408 | ● | | | | | |
| RE 40, 150 W | 142 | GP 52, 4.0 - 30 Nm | 318 | AB 28 | 408 | ● | | | | | |

## Technical Data

| | |
|---|---|
| Supply voltage $V_{CC}$ | 5 V ± 10% |
| Output signal | TTL compatible |
| Phase shift Φ | 90°e ± 45°e |
| Signal rise time (typically, at $C_L$ = 25 pF, $R_L$ = 2.7 kΩ, 25 °C) | 180 ns |
| Signal fall time (typically, at $C_L$ = 25 pF, $R_L$ = 2.7 kΩ, 25 °C) | 40 ns |
| Index pulse width (nominal) | 90°e |
| Operating temperature range | -40…+100 °C |
| Moment of inertia of code wheel | ≤ 0.6 gcm² |
| Max. angular acceleration | 250000 rad s⁻² |
| Output current per channel | min. -1 mA, max. 5 mA |

The index signal I is synchronized with channel A or B.

## Pin Allocation

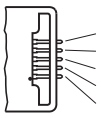

| Encoder | Description | Pin no. from 3409.506 |
|---|---|---|
| Pin 5 | Channel B | 1 |
| Pin 4 | $V_{CC}$ | 2 |
| Pin 3 | Channel A | 3 |
| Pin 2 | Channel I | 4 |
| Pin 1 | GND | 5 |

## Connection example

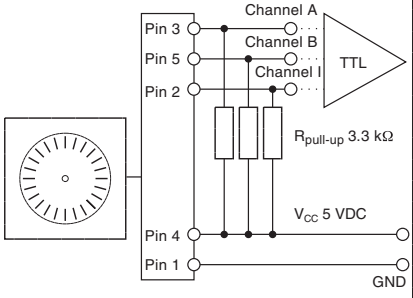


Ambient temperature range $\vartheta_U$ = 25 °C

# Encoder HEDS 5540 500 CPT, 3 Channels

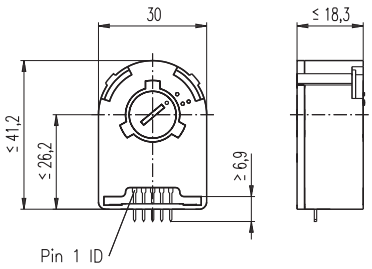


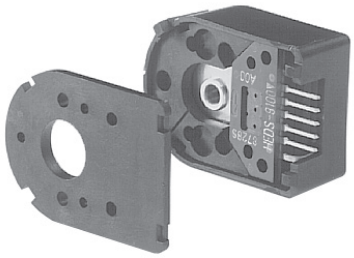

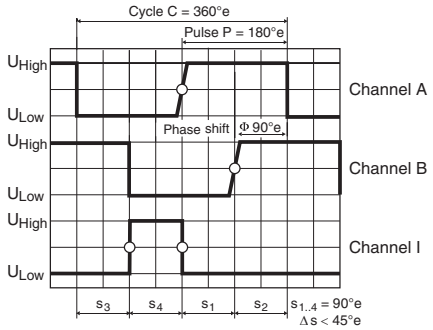


Direction of rotation cw (definition cw p. 106)

Stock program
Standard program
Special program (on request)

| Part Numbers | 110511 | 110513 | 110515 | 110517 |
|---|---|---|---|---|
| **Type** | | | | |
| Counts per turn | 500 | 500 | 500 | 500 |
| Number of channels | 3 | 3 | 3 | 3 |
| Max. operating frequency (kHz) | 100 | 100 | 100 | 100 |
| Max. speed (rpm) | 12000 | 12000 | 12000 | 12000 |
| Shaft diameter (mm) | 3 | 4 | 6 | 8 |

## maxon Modular System

| + Motor | Page | + Gearhead | Page | + Brake | Page | Overall length [mm] / ● see Gearhead | | | |
|---|---|---|---|---|---|---|---|---|---|
| RE 25, 20 W | 136 | | | | | 63.8 | | | |
| RE 25, 20 W | 136 | GP 26, 0.75 - 2.0 Nm | 301 | | | ● | | | |
| RE 25, 20 W | 136 | GP 32, 0.75 - 4.5 Nm | 303 | | | ● | | | |
| RE 25, 20 W | 136 | GP 32, 0.75 - 6.0 Nm | 304/307 | | | ● | | | |
| RE 25, 20 W | 136 | KD 32, 1.0 - 4.5 Nm | 312 | | | ● | | | |
| RE 25, 20 W | 136 | GP 32 S | 334-336 | | | ● | | | |
| RE 25, 20 W | 136 | | | AB 28 | 408 | 94.3 | | | |
| RE 25, 20 W | 136 | GP 22, 0.5 Nm | 293 | | | ● | | | |
| RE 25, 20 W | 136 | GP 26, 0.75 - 2.0 Nm | 301 | AB 28 | 408 | ● | | | |
| RE 25, 20 W | 136 | GP 32, 0.75 - 4.5 Nm | 303 | AB 28 | 408 | ● | | | |
| RE 25, 20 W | 136 | GP 32, 0.75 - 6.0 Nm | 304/307 | AB 28 | 408 | ● | | | |
| RE 25, 20 W | 136 | KD 32, 1.0 - 4.5 Nm | 312 | AB 28 | 408 | ● | | | |
| RE 25, 20 W | 136 | GP 32 S | 334-336 | AB 28 | 408 | ● | | | |
| RE 50, 200 W | 143 | | | | | | | | 128.7 |
| RE 50, 200 W | 143 | GP 52, 4 - 30 Nm | 319 | | | | | | ● |
| RE 50, 200 W | 143 | GP 62, 8 - 50 Nm | 320 | | | | | | ● |
| RE 65, 250 W | 144 | | | | | | | | 157.3 |
| RE 65, 250 W | 144 | GP 81, 20 - 120 Nm | 321 | | | | | | ● |
| A-max 26 | 162-168 | | | | | 63.1 | | | |
| A-max 26 | 162-168 | GP 26, 0.75 - 4.5 Nm | 301 | | | ● | | | |
| A-max 26 | 162-168 | GS 30, 0.07 - 0.2 Nm | 302 | | | ● | | | |
| A-max 26 | 162-168 | GP 32, 0.75 - 4.5 Nm | 303 | | | ● | | | |
| A-max 26 | 162-168 | GP 32, 0.75 - 6.0 Nm | 304/308 | | | ● | | | |
| A-max 26 | 162-168 | GS 38, 0.1 - 0.6 Nm | 313 | | | ● | | | |
| A-max 26 | 162-168 | GP 32 S | 334-336 | | | ● | | | |
| A-max 32 | 170/172 | | | | | | 82.3 | | |
| A-max 32 | 170/172 | GP 32, 0.75 - 6.0 Nm | 303-308 | | | | ● | | |
| A-max 32 | 170/172 | GS 38, 0.1 - 0.6 Nm | 313 | | | | ● | | |
| A-max 32 | 170/172 | GP 32 S | 334-336 | | | | ● | | |
| EC 32, 80 W | 214 | | | | | | 78.4 | | |
| EC 32, 80 W | 214 | GP 32, 0.75 - 6.0 Nm | 303-309 | | | | ● | | |
| EC 32, 80 W | 214 | GP 32 S | 334-336 | | | | ● | | |
| EC 40, 170 W | 215 | | | | | | | 103.4 | |
| EC 40, 170 W | 215 | GP 42, 3.0 - 15 Nm | 314 | | | | | ● | |
| EC 40, 170 W | 215 | GP 52, 4.0 - 30 Nm | 318 | | | | | ● | |

## Technical Data

| | |
|---|---|
| Supply voltage $V_{CC}$ | 5 V ± 10% |
| Output signal | TTL compatible |
| Phase shift Φ | 90°e ± 45°e |
| Signal rise time (typically, at $C_L$ = 25 pF, $R_L$ = 2.7 kΩ, 25 °C) | 180 ns |
| Signal fall time (typically, at $C_L$ = 25 pF, $R_L$ = 2.7 kΩ, 25 °C) | 40 ns |
| Index pulse width | 90°e |
| Operating temperature range | -40…+100 °C |
| Moment of inertia of code wheel | ≤ 0.6 gcm² |
| Max. angular acceleration | 250000 rad s⁻² |
| Output current per channel | min. -1 mA, max. 5 mA |

The index signal I is synchronized with channel A or B.

## Pin Allocation

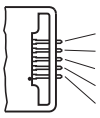

| Encoder | Description | Pin no. from 3409.506 |
|---|---|---|
| Pin 5 | Channel B | 1 |
| Pin 4 | $V_{CC}$ | 2 |
| Pin 3 | Channel A | 3 |
| Pin 2 | Channel I | 4 |
| Pin 1 | GND | 5 |

## Connection example

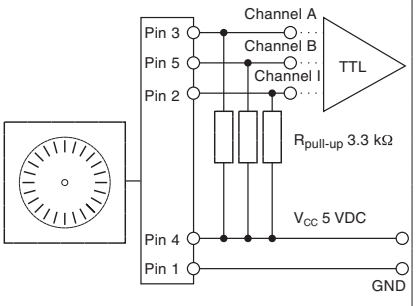


Ambient temperature range $\vartheta_U$ = 25 °C

# RE 36 ∅36 mm, Escobillas de grafito, 70 Vatios



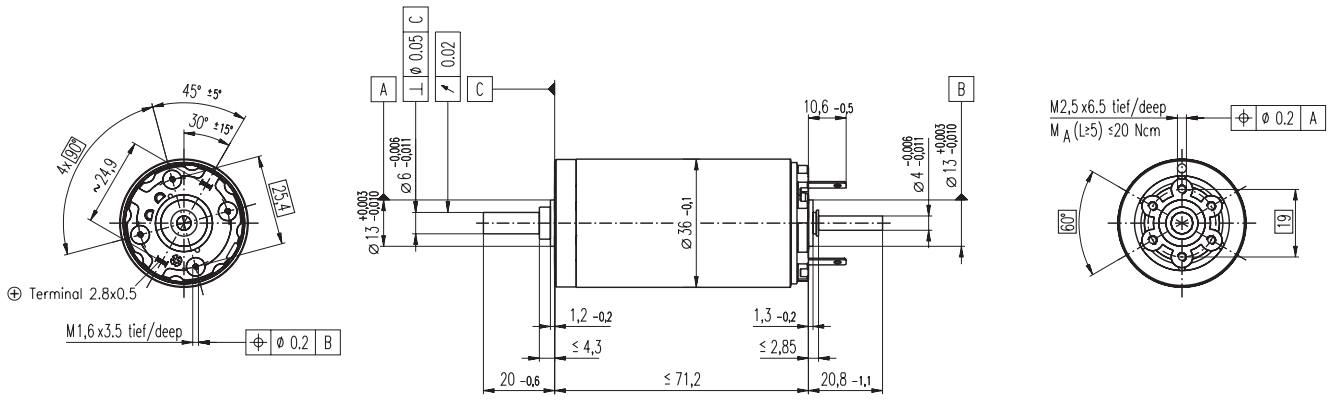


**M 1:2**

Programa Stock
Programa Estándar
Programa Especial (¡previo encargo!)

## Números de Referencia

| | | | 118797 | 118798 | 118799 | 118800 | 118801 | 118802 | 118803 | 118804 | 118805 | 118806 | 118807 | 118808 | 118809 | 118810 |
|---|---|---|---|---|---|---|---|---|---|---|---|---|---|---|---|---|
| **Datos del motor** | | | | | | | | | | | | | | | | |
| 1 | Potencia nominal asignada | W | 70 | 70 | 70 | 70 | 70 | 70 | 70 | 70 | 70 | 70 | 70 | 70 | 70 | 70 |
| 2 | Tensión nominal | Volt | 18.0 | 24.0 | 32.0 | 42.0 | 42.0 | 48.0 | 48.0 | 48.0 | 48.0 | 48.0 | 48.0 | 48.0 | 48.0 | 48.0 |
| 3 | Velocidad en vacío | rpm | 6610 | 6210 | 6790 | 7020 | 6340 | 6420 | 5220 | 4320 | 3450 | 2830 | 2280 | 1780 | 1420 | 1180 |
| 4 | Par de arranque | mNm | 730 | 783 | 832 | 865 | 786 | 785 | 627 | 504 | 403 | 326 | 258 | 198 | 158 | 127 |
| 5 | Relación velocidad / par | rpm / mNm | 9.23 | 8.05 | 8.27 | 8.19 | 8.14 | 8.25 | 8.41 | 8.65 | 8.67 | 8.80 | 8.96 | 9.17 | 9.21 | 9.51 |
| 6 | Corriente en vacío | mA | 153 | 105 | 89 | 70 | 61 | 55 | 42 | 33 | 25 | 20 | 15 | 12 | 9 | 7 |
| 7 | Corriente de arranque | A | 28.6 | 21.5 | 18.7 | 15.3 | 12.6 | 11.1 | 7.22 | 4.80 | 3.06 | 2.04 | 1.30 | 0.784 | 0.501 | 0.334 |
| 8 | Resistencia en bornes | Ohm | 0.628 | 1.11 | 1.71 | 2.75 | 3.35 | 4.32 | 6.65 | 10.00 | 15.7 | 23.5 | 36.8 | 61.3 | 95.8 | 144 |
| 9 | Máx. velocidad permitida | rpm | 8200 | 8200 | 8200 | 8200 | 8200 | 8200 | 8200 | 8200 | 8200 | 8200 | 8200 | 8200 | 8200 | 8200 |
| 10 | Máx. corriente en continuo | A | 3.18 | 2.44 | 1.99 | 1.59 | 1.44 | 1.27 | 1.03 | 0.847 | 0.679 | 0.556 | 0.445 | 0.346 | 0.277 | 0.226 |
| 11 | Máx. par permanente | mNm | 81 | 88.8 | 88.5 | 89.8 | 90.4 | 90.1 | 89.8 | 89.0 | 89.2 | 88.8 | 88.1 | 87.3 | 87.2 | 85.8 |
| 12 | Máx. potencia útil a tensión nominal | W | 123 | 125 | 146 | 157 | 129 | 131 | 84.9 | 56.4 | 36.0 | 23.9 | 15.2 | 9.09 | 5.78 | 3.82 |
| 13 | Máx. rendimiento | % | 84 | 85 | 86 | 86 | 86 | 86 | 85 | 84 | 82 | 81 | 79 | 77 | 75 | 72 |
| 14 | Constante de par | mNm / A | 25.5 | 36.4 | 44.5 | 56.6 | 62.6 | 70.7 | 86.9 | 105 | 131 | 160 | 198 | 253 | 315 | 380 |
| 15 | Constante de velocidad | rpm / V | 375 | 263 | 215 | 169 | 152 | 135 | 110 | 90.9 | 72.7 | 59.8 | 48.2 | 37.8 | 30.3 | 25.1 |
| 16 | Constante de tiempo mecánica | ms | 6 | 6 | 6 | 6 | 6 | 6 | 6 | 6 | 6 | 6 | 6 | 6 | 6 | 6 |
| 17 | Inercia del rotor | gcm² | 60.2 | 67.7 | 65.2 | 65.4 | 65.6 | 64.6 | 63.3 | 61.5 | 61.3 | 60.3 | 59.2 | 57.8 | 57.5 | 55.7 |
| 18 | Inductancia en bornes | mH | 0.10 | 0.20 | 0.30 | 0.49 | 0.60 | 0.76 | 1.15 | 1.68 | 2.62 | 3.87 | 5.96 | 9.70 | 15.10 | 21.90 |
| 19 | Resistencia térmica carcasa / ambiente | K / W | 6.4 | 6.4 | 6.4 | 6.4 | 6.4 | 6.4 | 6.4 | 6.4 | 6.4 | 6.4 | 6.4 | 6.4 | 6.4 | 6.4 |
| 20 | Resistencia térmica rotor / carcasa | K / W | 3.4 | 3.4 | 3.4 | 3.4 | 3.4 | 3.4 | 3.4 | 3.4 | 3.4 | 3.4 | 3.4 | 3.4 | 3.4 | 3.4 |
| 21 | Constante de tiempo térmica de bobinado | s | 38 | 43 | 41 | 41 | 41 | 41 | 40 | 39 | 39 | 38 | 37 | 36 | 36 | 35 |

## Especificaciones

- Juego axial 0.05 - 0.15 mm
- Carga máx. en el **rodamiento a bolas**
  axial (dinámica)
  sin pretensado 5.6 N
  pretensado 2.4 N
  radial (a 5 mm de la brida) 28 N
  Fuerza de empuje a presión (estática) 110 N
  (idem, con eje sostenido) 1200 N
- Juego radial en **rodamiento a bolas** 0.025 mm
- Temperatura ambiente -20 ... +100°C
- Máx. temperatura del rotor +125°C
- Número de delgas del colector 13
- Peso del motor 350 g
- Imàn permanente de 2 polos
- Los datos de la tabla son valores nominales. Para las tolerancias aplicables (ver página 43) y para detalles adicionales solicite nuestro servicio de asistencia por ordenador.

⚠ Para este motor, las tolerancias pueden variar de la especificación estándar.

## Rango de funcionamiento

Leyenda Detalles en página 49

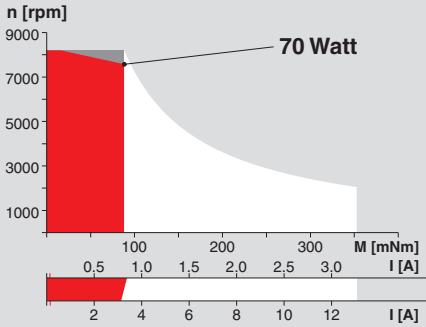


**Rango recomendado de funcionamiento**

**Funcionamiento continuo**
Teniendo en cuenta los valores de resistencia térmica antes mencionados (líneas 19 y 20). El rotor alcanzará la máxima temperatura durante funcionamiento continuo a 25°C de temperatura ambiente = límite térmico.

**Funcionamiento intermitente**
El motor puede ser sobrecargado durante cortos períodos (cíclicamente).

118804 Motor con bobinado de alta resistencia
118797 Motor con bobinado de baja resistencia

## Sistema Modular maxon

Esquema general en página 17 - 21

**Reductor Planetario**
∅32 mm
0.75 - 4.5 Nm
Detalles página 213

**Reductor Planetario**
∅32 mm
1.0 - 6.0 Nm
Detalles página 214

**Reductor Planetario**
∅32 mm
0.4 - 2.0 Nm
Detalles página 216

**Reductor Planetario**
∅42 mm
3 - 15 Nm
Detalles página 218

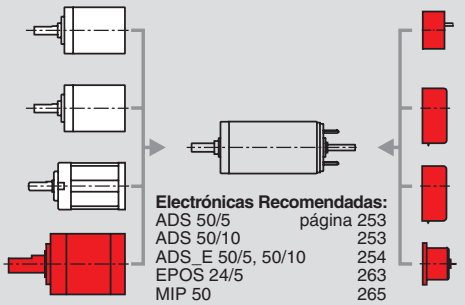

**Electrónicas Recomendadas:**
ADS 50/5 página 253
ADS 50/10 253
ADS_E 50/5, 50/10 254
EPOS 24/5 263
MIP 50 265
**Notas** 17

**Encoder Digital MR**
256 - 1024 ppv,
3 canales
Detalles página 233

**Encoder Digital HP HEDS 5540**
500 ppv, 3 canales
Detalles pág. 236

**Encoder Digital HP HEDL 5540**
500 ppv, 3 canales
Detalles página 238

**Tacodinamos CC**
∅22 mm
0.52 V
Detalles página 246

# **Encoder HEDL 5540,** 500 ppv, 3 canales, con line driver RS 422

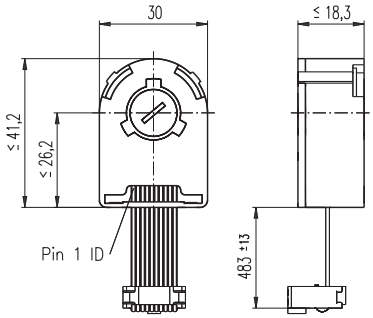


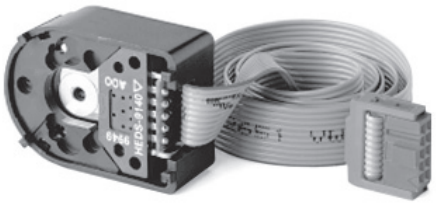

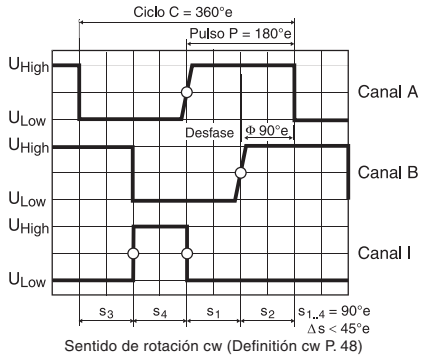


Sentido de rotación cw (Definitión cw P. 48)

Programa Stock
Programa Estándar
Programa Especial (previo encargo)

| Números de Referencia | | | |
|---|---|---|---|
| 110512 | 110514 | 110516 | 110518 |

| Tipo | | | | |
|---|---|---|---|---|
| Número de pulsos por vuelta | 500 | 500 | 500 | 500 |
| Número de canales | 3 | 3 | 3 | 3 |
| Máx. frecuencia de funcionamiento (kHz) | 100 | 100 | 100 | 100 |
| Máx. velocidad (rpm) | 12000 | 12000 | 12000 | 12000 |
| Diámetro de eje (mm) | 3 | 4 | 6 | 8 |



## Sistema Modular maxon

| + Motor | Página | + Reductor | Página | + Freno | Página | Longitud total [mm] / ● ver reductor | | | |
|---|---|---|---|---|---|---|---|---|---|
| RE 50, 150 W | 83 | | | | | | | | 128.7 |
| RE 50, 150 W | 83 | GP 52, 4 - 30 Nm | 242 | | | | | | ● |
| RE 50, 150 W | 83 | GP 62, 8 - 50 Nm | 243 | | | | | | ● |
| RE 65, 250 W | 84 | | | | | | | | 157.3 |
| RE 65, 250 W | 84 | GP 81, 20 - 120 Nm | 244 | | | | | | ● |
| EC 32, 80 W* | 153 | | | | | | 78.4 | | |
| EC 32, 80 W* | 153 | GP 32, 0.75 - 4.5 Nm | 230 | | | | ● | | |
| EC 32, 80 W* | 153 | GP 32, 0.75 - 6.0 Nm | 232/234 | | | | ● | | |
| EC 32, 80 W* | 153 | GP 32 S | 249-251 | | | | ● | | |
| EC 40, 120 W* | 154 | | | | | | | 88.4 | |
| EC 40, 120 W* | 154 | GP 42, 3.0 - 15 Nm | 238 | | | | | ● | |
| EC 40, 120 W* | 154 | GP 52, 4.0 - 30 Nm | 241 | | | | | ● | |
| EC-max 30, 40 W | 166 | | | | | | 62.6 | | |
| EC-max 30, 40 W | 166 | GP 32, 1 - 6 Nm | 234 | | | | ● | | |
| EC-max 30, 40 W | 166 | | | AB 20 | 316 | | 101.7 | | |
| EC-max 30, 40 W | 166 | GP 32, 1 - 6 Nm | 234 | AB 20 | 316 | | ● | | |
| EC-max 30, 40 W | 166 | GP 32 S | | | | | ● | | |
| EC-max 30, 40 W | 166 | GP 32, 4.0 - 8.0 Nm | 235 | | | | | | |
| EC-max 30, 60 W | 167 | | | | | | 84.6 | | |
| EC-max 30, 60 W | 167 | GP 32, 4.0 - 8.0 Nm | 235 | | | | | | |
| EC-max 30, 60 W | 167 | GP 42, 3 - 15 Nm | 239 | | | | ● | | |
| EC-max 30, 60 W | 167 | | | AB 20 | 316 | | 123.7 | | |
| EC-max 30, 60 W | 167 | GP 42, 3 - 15 Nm | 239 | AB 20 | 316 | | ● | | |
| EC-max 40, 70 W | 168 | | | | | | | 81.4 | |
| EC-max 40, 70 W | 168 | GP 42, 3 - 15 Nm | 239 | | | | | ● | |
| EC-max 40, 70 W | 168 | | | AB 28 | 317 | | | 121.4 | |
| EC-max 40, 70 W | 168 | GP 42, 3 - 15 Nm | 239 | AB 28 | 317 | | | ● | |
| EC-max 40, 120 W | 169 | | | | | | | 111.4 | |
| EC-max 40, 120 W | 169 | GP 52, 4 - 30 Nm | 242 | | | | | ● | |
| EC-max 40, 120 W | 169 | | | AB 28 | 317 | | | 151.4 | |
| EC-max 40, 120 W | 169 | GP 52, 4 - 30 Nm | 242 | AB 28 | 317 | | | ● | |

* Conexión siehe Página 268

## Datos técnicos

| | |
|---|---|
| Tensión de alimentación | 5 V ± 10 % |
| Señal de salida | EIA Standard RS 422 |
| Drivers integrados: | DS26LS31 |
| Desfase Φ | 90°e ± 45°e |
| Tiempo del frente de subida (típico con $C_L$ = 25 pF, $R_L$ = 2.7 kΩ, 25°C) | 180 ns |
| Tiempo del frente de bajada (típico con $C_L$ = 25 pF, $R_L$ = 2.7 kΩ, 25°C) | 40 ns |
| Anchura de pulso index | 90°e |
| Rango de temperaturas | -40 ... +100°C |
| Momento de la inercia de la rueda de código | ≤ 0.6 gcm² |
| Máx. aceleración angular | 250 000 rad s⁻² |
| Corriente de salida por canal | min. -20 mA, max. 20 mA |
| Option | 1000 ppv, 2 canales |

La señal del canal index I es sincronizada con el canal A y con el B.

## Conexión para motor RE 75

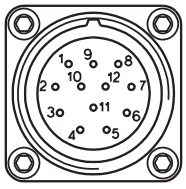


**Tipo ensanchado del conector**
**Tipo SOURIAU 8GM-QL2-12P**
1 $V_{CC}$
2 N.C. (no conectar)
3 GND
4 N.C. (no conectar)
5 Canal I (Index)
6 Canal $\overline{I}$
7 Canal B
8 Canal $\overline{B}$
9 Canal A
10 Canal $\overline{A}$
11 N.C. (no conectar)
12 N.C. (no conectar)
Conectores recomendados
Tipo SOURIAU 8GM-DM2-12S (metal, salida recta:
**maxon** N° de artículo 2675.538) o
8G-V2-12S (plástico, ángulo 90°:
**maxon** N° de artículo 2675.539)

## Ejemplo de conexión

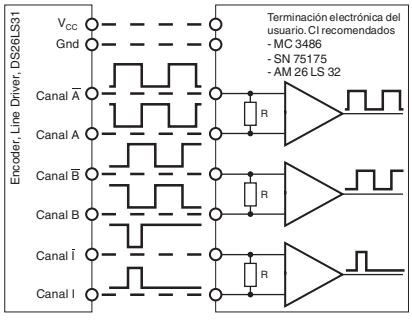


Resistencia en bornes R = típica 120 Ω